Seasonal characteristics of biogenic secondary organic aerosols over Chichijima Island in the western North Pacific: Impact of biomass burning activity in East Asia

Santosh Kumar Verma,[1,2] Kimitaka Kawamura,[1,3,*] Dhananjay Kumar Deshmukh,[1,3] Md. Mozammel Haque,[1, a] Chandra Mouli Pavuluri[4]

[1]Institute of Low Temperature Science, Hokkaido University, Sapporo 060-0819, Japan
[2]State Forensic Science Laboratory, Home Department, Government of Chhattisgarh, Raipur 491001, India
[3] Chubu Institute for Advanced Studies, Chubu University, Kasugai 487-8501, Japan
[a] Now at Yale-NUIST Center on Atmospheric Environment, Department of Applied Meteorology, Nanjing University of Information Science and Technology, Nanjing 210044, China
[4]Institute of Surface-Earth System Science, Tianjin University, Tianjin 300072, China

**Corresponding author:* Kimitaka Kawamura
E-mail: kkawamura@isc.chubu.ac.jp
Tel.: +81-568-51-9330

Key Points:

1. We report 3-year observations of biogenic secondary organic aerosols (BSOAs) at Chichijima Island in the western North Pacific.
2. Monoterpene oxidation products are the significant sources for BSOAs, followed by isoprene and β-caryophyllene oxidation products in Chichijima aerosols.
3. High-NOx BSOA tracers (2-MGA, 3-HGA, and 3-MBTCA) are influenced by a long-range transport of anthropogenic air masses and low-NOx BSOA tracers (2-MTLs and C5-alkene triols) are produced mainly by the oxidation of locally emitted isoprene.
4. Biomass burning aerosols contribute to β-caryophyllene-derived BSOA tracer by atmospheric oxidation during long-range transport from the Asian continent over the western North Pacific.

Abstract

To better understand the formation processes of biogenic secondary organic aerosols (SOAs) over remote oceanic regions, aerosol samples were collected from 2010 to 2012 at Chichijima Island in the western North Pacific (WNP). The samples were analyzed by gas chromatography-mass spectrometry for SOA tracers, which are produced by the photochemical oxidation of biogenic volatile organic compounds (BVOCs), including isoprene, monoterpene and sesquiterpene. Although no seasonal trend was identified for the isoprene-derived SOA tracers, we observed higher levels of the monoterpene-derived and sesquiterpene-derived SOA tracers in winter/spring and lower levels in summer/autumn. We found a significant correlation (r = 0.87) of β-caryophyllinic acid with levoglucosan, the latter being a specific tracer of biomass burning (BB). This suggests that the β-caryophyllene accumulated in higher plants is evaporated by BB followed by atmospheric oxidation during long-range transport from the Asian continent over the WNP. The biogenic secondary organic carbon concentration estimated using a tracer-based approach ranged from 0.11–174 ngC m^{-3} (avg. 34.8±38.2 ngC m^{-3}), accounting for 0.02–32.0% (avg. 6.11±6.42%) of the measured organic carbon. Our results indicate that SOAs are formed by the photooxidation of BVOCs. The backward trajectories of air masses further support their transport from the central Pacific during mid-spring to mid-autumn, whereas BB aerosols are transported from the Asian continent during mid-autumn to mid-spring over the WNP. Positive matrix factorization analyses of the SOA tracers suggest that organic aerosols of Chichijima are mostly related to BVOC emissions, with BB's additional contributions especially in winter and spring. (248)

Keywords: Biogenic SOA tracers, biomass burning, continental influence, remote marine aerosols.

1. Introduction

Atmospheric aerosols are derived from various natural and anthropogenic sources (Robinson et al., 2006; de Gouw and Jimenez, 2009). Primary aerosols are directly emitted from continents, oceans, arid regions, volcanic eruptions, fossil fuel combustion, and biomass burning (BB). Conversely, secondary aerosols are formed by photochemical reactions via gas-to-particle conversion in the atmosphere (Hallquist et al., 2009). Secondary organic aerosols (SOAs) are abundant, representing one of the most important components of carbonaceous aerosols that significantly affect the atmospheric radiation budget, both directly by scattering sunlight and indirectly by acting as cloud condensation nuclei (CCN) (Kanakidou et al., 2005). Considerable efforts have been devoted in recent decades to developing an understanding of SOA formation by the photooxidation of volatile organic compounds (VOCs) of anthropogenic and biogenic origin (Kavouras et al., 1998). Biogenic VOCs (BVOCs) are emitted from terrestrial vegetation and marine biota (Guenther et al., 2006).

Guenther et al. (1995) estimated the annual global emission of BVOCs to be 1150 TgC yr^{-1}, of which isoprene and monoterpenes accounted for 44% and 11%, respectively. Similarly, Piccot et al. (1992) reported the emission of 110 TgC yr^{-1} of anthropogenic VOCs (AVOCs), which is one order of magnitude lower than that of BVOCs. Hallquist et al. (2009) reported the global production of SOAs from BVOCs to be 9–910 TgC yr^{-1}. The contribution of BVOCs to SOA formation is much greater (8–40 Tg yr^{-1}) than that of AVOCs (0.3 to 1.8 Tg yr^{-1}) (Intergovernmental Panel on Climate Change, 2001). The emissions of BVOCs followed by SOA formation are expected to have a significant impact on the chemical composition and physical properties of tropospheric aerosols and thus climate change (Fowler et al., 2009). Although the AVOC contribution to SOA formation frequently exceeds 50% in urban areas due to the influence of human activities (Ding et al., 2012; von Schneidemesser et al., 2009), it is likely much smaller in the remote marine atmosphere.

The global production of SOAs from marine sources has been considered less important than from terrestrial sources. Meskhidze and Nenes (2006) suggested that marine phytoplankton could be an emission source of BVOCs and SOA formation. However, studies of the oxidation products of BVOCs in the remote marine atmosphere are limited in number. We note that remote marine aerosols would provide a unique opportunity to examine the atmospheric chemistry of BVOCs due to their being so far away from the anthropogenic sources on the continent. A potential source of SOAs in the free troposphere has been reported

to be the atmospheric oxidation of long-lived VOCs (Heald et al., 2005). Isoprene was included as an SOA precursor in a global model developed by Henze and Seinfeld (2006). Studies on SOA formation are essential for understanding the aerosol-cloud-climate system over the remote oceans (Meskhidze and Nenes, 2006).

The authors of several chamber studies have reported the anthropogenic influence on the formation of biogenic SOAs (BSOAs). Ding et al. (2014) found NO_x levels to significantly influence the concentrations of BSOA tracers in the atmosphere. Surratt et al. (2006) and Zhang et al. (2011) demonstrated that 2-methyltetrols are most likely generated under low-NO_x and high relative humidity (RH) conditions, whereas 2-methylglyceric acid is generated under high-NO_x and low RH conditions. Surratt et al. (2010) proposed that high-NO_x and low RH levels affected the formation of C_5-alkene triols. The results of chamber experiments conducted by Claeys et al. (2007) and Szmigielski et al. (2007) demonstrated the formation of 3-hydroxyglutaric acid and 3-methyl-1,2,3-butanetricarboxylic acid under UV-radiation in the presence of NO_x. Similarly, it is assumed that the anthropogenic NO_x emitted from the Asian continent is transported together with anthropogenic aerosols to Chichijima Island in the western North Pacific (WNP) (Boreddy et al., 2015). Under favorable meteorological conditions, NO_x may affect the seasonal concentrations and formation mechanisms of BSOA tracers over the remote ocean.

The vehicular emissions and BB in the East Asian countries are the primary sources of NO_x, which might be significantly transported to the downwind regions. The anthropogenic nitric oxide (NO) reacts with O_3 to form NO_2 and subsequently converts to nitrate (NO_3) radicals. The long lifetime of VOCs and their oxidation by photolabile NO_3 provide additional pathways for SOA formation, which is enhanced under high-NO_x conditions (Hoyle et al., 2011). Hoyle et al. (2007) reported a global modeling study where oxidation of SOA precursors by NO_3 in nighttime increases up to 21% of the global average SOA burden. Brown et al. (2009) reported that NO_3 initiated isoprene oxidation process increased up to 17% of SOA formation in the northeastern US. Ng et al. (2008) estimated that ~2 to 3 Tg of SOA yr^{-1} result from isoprene reaction with NO_3. Moreover, in the industrialized region, the average percentage increased to around 50–60%, suggesting the significance of anthropogenic emissions for the SOA formation pathway (Hoyle et al., 2007).

The East Asian monsoon significantly affects the regional climate and air quality of the outflow regions in the WNP (Yamamoto et al., 2011). Over Chichijima in the WNP, pristine

air masses usually travel from the Pacific Ocean in summer and autumn by easterly winds, whereas polluted air masses from the Asian continent are transported over the WNP in winter and spring by westerly winds (Chen et al., 2013). Verma et al. (2015) reported high concentrations of BB tracers in total suspended particulate (TSP) samples collected from Chichijima during winter and spring. Verma et al. (2018) discussed the influence of long-range atmospheric transport on the seasonal distributions of sugar components in Chichijima aerosols. A long-term (2001–2012) study of TSP samples from Chichijima found NO_3^- to be more abundant in winter and spring than summer and autumn over the WNP (Boreddy et al., 2015). The above studies demonstrate that atmospheric circulation and wind patterns control atmospheric aerosols seasonal sources and compositions over the Pacific Ocean.

In addition to continental emissions, followed by long-range atmospheric transport the marine atmosphere is also affected by oceanic emissions. Therefore, it is essential to investigate the SOA tracers in remote marine aerosols to determine their origin and impacts on the regional and global climates. In this study, we analyzed TSP samples collected from Chichijima to determine the molecular characteristics of the SOA tracers, and their abundances and sources over the WNP. Here, we discuss the influence of the local meteorology, atmospheric circulations, and long-range atmospheric transport of BVOCs and pollutants on the abundance of SOAs in Chichijima aerosols. We performed a diagnostic mass concentration ratio analysis, a tracer-based approach, and a positive matrix factorization (PMF) analysis at annual and seasonal scales to explore the variations in SOA tracers concentrations and sources over the WNP.

2. Materials and Methods

2.1. Sampling Site and Aerosol Sample Collection

The sampling site (Chichijima: 27.06°N and 142.21°E) is located at the Ogasawara Downrange Station of the Japan Aerospace Exploration Agency (JAXA) on Chichijima Island (Figure 1). A detailed description of the sampling site is given in Kawamura et al. (2003). Briefly, Chichijima is a small remote island located in the WNP approximately 2000 km east of the Asian continent and 1000 km south of Tokyo, Japan. The total area of the island is 24 km^2, and its population is about 2000. The climate of Chichijima is classified as subtropical. The island is too far away from the Asian continent to receive monsoonal rainfall on the equator ward side of the Siberian High and too far south to be influenced by the Aleutian Low.

Figure 2 shows the monthly average values of the meteorological parameters over Chichijima Island during the campaign. Its climate is a humid year around. The monthly mean RH was found to be lowest in January 2011 (62%) and highest in June 2012 (89%), with an average of 77% during the study period. The monthly mean temperatures ranged from 7.8 °C in January to 34.1 °C in August (avg. 23.5 °C). More precipitation events were recorded at the sampling site between April and July and September and October. The total precipitation amounts were 1393, 942, and 1229 mm, respectively, in 2010, 2011, and 2012. A broad-leaved evergreen forest covers a large part of the island. The vegetation of Chichijima is characterized by rich endemic flora (75%) and short trees with sclerophyllous leaves on the ridge sites. The plants typically experience severe drought in July and early summer, especially on the ridge sites, due to low precipitation levels, high temperatures, and shallow volcanic soil. Typhoons also affect the climate and vegetation of Chichijima as these frequently occur from mid-summer to mid-autumn.

Detailed descriptions of the TSP samples collected at Chichijima Island are given in Mochida et al. (2010) and Chen et al. (2013). Briefly, a high-volume air sampler (Kimoto AS810A) was placed at JAXA's Ogasawara Downrange Station on Chichijima. The samples were collected on precombusted (450 °C for 6 h) quartz fiber filters at a flow rate of 1.0 m^3 min^{-1} on a weekly basis from January 2010 to December 2012. After sample collection, to prevent microbial activity and the loss of semi-VOCs from the samples, the individual filters were placed in a precombusted glass jar with a Teflon-lined screw cap and stored in a dark, cold room at −20 °C until analysis. In this study, a total of 171 filter samples were analyzed, including 17 field blanks.

2.2. Extraction and Derivatization of Samples

Approximately 21 cm^2 of each of the sample filters were extracted with a dichloromethane and methanol mixture (2:1) under ultrasonication. The extracts were filtered through a Pasteur pipette packed with precombusted quartz wool to remove filter debris and then concentrated in a rotary evaporator under vacuum and dried by nitrogen blowdown. To convert the hydroxy groups into corresponding trimethylsilyl (TMS) ethers and the carboxyl groups into TMS esters, the extracts were then derivatized with N,O-bis(trimethylsilyl)trifluoroacetamide (BSTFA) with 1% TMS chloride in the presence of 10 μL of pyridine in a 1.5 mL precombusted glass vial sealed with a Teflon-lined screw cap at 70 °C

for three hours. More details regarding the extraction and derivatization procedures are reported in Fu et al. (2008).

2.3. Gas Chromatography–Mass Spectrometry Determination of SOA Tracers

Before injection into a gas chromatograph-mass spectrometer (GC-MS), the derivatized fraction was diluted with *n*-hexane containing an internal standard of *n*-C_{13} alkane (1.43 ng μL^{-1}). GC-MS analyses of samples were performed on an Agilent model 7890 GC coupled to an Agilent model 5975 mass selective detector (MSD). The mass spectrometer was operated in the electron ionization (EI) mode at 70 eV and scanned in the *m/z* range 40–650 Da. The GC was equipped with a split/splitless injector and a DB-5MS fused silica capillary column (30 m × 0.25 mm in diameter, 0.25 μm film thickness). The GC oven temperature was programmed to be 50 °C for 2 min at a rate of 15 °C min^{-1} from 50 to 120 °C, then from 120 to 305 °C at 5 °C min^{-1}. The final isotherm holds at 305 °C for 15 min. Helium was used as the carrier gas at a flow rate of 1.0 mL min^{-1}. The sample was injected on a splitless mode at 280 °C injector temperature. GC-MS data were acquired and processed with an Agilent GC/MSD ChemStation software.

The compound masses were also compared using the relative response factors determined by the injection of authentic standards and those reported in the literature and library texts. The average response factors of internal standard calibration for the surrogates were average of 2.18. In total 11 BSOA tracers including 2-methylthreitol (2-MTL_1), 2-methylerythritol (2-MTL_2), 2-methylglyceric acid (2-MGA), cis-2-methyl-1,3,4-trihydroxy-1-butene, 3-methyl-2,3,4-trihydroxy-1-butene, trans-2-methyl-1,3,4-trihydroxy-1-butene (C_5-alkene triols), *cis*-pinonic (PNA), pinic acids (PA), 3-methyl-1,2,3-butanetricarboxylic acid (3-MBTCA), 3-hydroxyglutaric acid (3-HGA) and *β*-caryophyllinic acid were detected in Chichijima aerosol.

2.4. Quality Assurance and Quality Control

A total ion chromatogram (TIC) provides a reliable approach for tracer quantification in the absence of authentic standards. Kleindienst et al. (2007) used TMS derivatives of ketopinic acid for quantitative estimation of SOA tracers because no standards were available for the majority of the compounds. In this study, GC-MS response factors were determined using authentic standards of PNA, PA, 3-HGA and meso-erythritol to quantify SOA tracers. The concentrations of 2-MTLs (2-MTL_1 and 2-MTL_2), 2-MGA, and C_5-alkene triols were

estimated using the response factor of meso-erythritol (Wang et al., 2008; Kourtchev et al., 2008), whereas the response factor of PA was used to quantify 3-MBTCA and *β*-caryophyllinic acid (Jaoui et al., 2007; Ding et al., 2011) due to the unavailability of commercial standards. The EI spectrum and TIC with the retention time, observed MS fragments and relative ratio of fragments of each tracers compounds were presented in Figures S1 and S2a–S2k, which supported a correct identification of the SOA tracers. The ionization and mass fragmentation of target SOA tracers are different from the surrogate standards. Therefore, the substantial uncertainties caused by different surrogate standards were estimated based on the method described in Stone et al. (2012).

The recoveries of authentic standards or surrogates that were spiked onto a precombusted quartz fiber filters (n = 3) were 90 ± 5% for 3-HGA, 93 ± 4% for meso-erythritol, 89 ± 3% for PNA, and 78 ± 4% for PA. Based on the duplicate analysis, the analytical errors in the detected compounds concentrations were determined to be within 10%. Field blanks were collected every two months during the campaign at the observation site, which was analyzed as the real samples. The measured SOA tracers were not detected in these field blanks. The method detection limits (MDL) for 3-HGA, meso-erythritol, PNA acid and PA were 3.2, 4.3, 1.2 and 2.6 pg m^{-3}, respectively, under a typical sampling volume of 4500 m^3.

2.5. Estimation of Measurement Uncertainty

The standards for PNA, PA and 3-HGA are available commercially among all the measured SOA tracers in this study. Hence, the additional error introduces for the quantification while using surrogate standards in the analytical measurements. The uncertainties in the measurements of SOA tracers were calculated by the following equation developed by Stone et al. (2012):

$$E_A = \sqrt{E_{FB}^2 + E_R^2 + E_Q^2} \qquad \text{(Eqn. - 01)}$$

where E_A is an error in analyte measurement, E_{FB} is the standard deviation of the field blank, E_R is the error in spike recovery, and E_Q is the error from surrogate quantification. E_{FB} was 0 in this study because no target compounds were detected in the field blanks. The spike recoveries of surrogate standards were used to estimate the E_R of SOA tracers, ranging from 2 to 23%. An empirical approach was developed by Stone et al. (2012) to estimate E_Q based on the

homologous series of atmospherically relevant compounds. The relative error introduced by each carbon atom (E*n*) was estimated to be 15%, each oxygenated functional group (E*f*) to be 10%, and alkenes (E*d*) to be 60%. The errors introduced from surrogate quantification are treated as an additive and are calculated with Eqn. - 02,

$$E_Q = E_n \Delta n + E_f \Delta f + E_d \Delta d \qquad \text{(Eqn. - 02)}$$

where Δn is the difference in carbon atom number between a surrogate and an analyte, Δf is the difference in the oxygen-containing functional group between a surrogate and an analyte, Δd is the difference in alkene functionality between a surrogate and an analyte. The quantification errors (E_Q) were then propagated with the other source of measurement uncertainty using Eqn. - 01 were ranged from 15% (2-MTLs) to 140% (*β*-caryophyllinic acid) in this study. The quantification errors (E_Q) yield the following uncertainties (E_A) for SOA tracers in this study were 20% for 2-MTLs, 25% for 2-MGA, 83% for C_5-alkene triols, 50% for 3-MBTCA, and 145% for *β*-caryophyllinic acid.

2.6. Air-mass Circulation and Back Trajectories

The five-day air-mass backward trajectories (AMBTs) arriving over the sampling site 500 m above ground level were computed for each sample using the Hybrid Single-Particle Lagrangian Integrated Trajectory (HYSPLIT) model developed by the National Oceanic and Atmospheric Administration (NOAA) Air Resources Laboratory (ARL) (Draxler and Rolph, 2013). Figure 3 shows the seasonal AMBTs for the samples collected at Chichijima. These trajectory-based observations show two significant pathways for the air masses that arrived in Chichijima, which indicate that the observation site is strongly affected by seasonal changes in the wind system. Trade winds, which are dominant from mid-spring to mid-autumn, transport clean and pristine marine air masses from the central Pacific. The westerly winds dominate from mid-autumn to mid-spring, bringing continental air masses enriched with pollutants including NO_x, dust, and anthropogenic aerosols emitted from East Asia and Eurasia (Kawamura et al., 2003; Simoneit et al., 2004; Wang et al., 2009).

Bourgeois and Bey (2011) reported global lifetimes of aerosol in the air are about five days by estimating the loss rate constant of tracers as 2.3×10^{-12} cm^3 $molec^{-1}$ s^{-1} at OH levels of 1×106 molecules cm^{-3}. According to the above study, five days lifetime was also assumed for SOA tracers in Chichijima aerosols; however, it may vary for a different environment. Therefore, considering the lifetime of SOA tracers is five days, we compute the five-day air-

mass backward trajectories arriving over the sampling site 500 m above ground level. Apart from the above study, detailed research is needed about the stability, degradation, and lifetime of the SOA tracers during long-range transport.

2.7. Positive Matrix Factorization (PMF) Analysis

Positive matrix factorization (PMF) is a powerful statistical tool for resolving the potential sources contributing to atmospheric particles (Paatero and Tapper, 1994). The uncertainties were calculated by using the measured ambient concentrations and method detection limits (MDLs). The measured concentrations of SOA tracers below or equal to the MDLs were replaced by half of the MDL, and associated uncertainties were set at five-sixths of the MDL [(5/6) × MDL] values of each sample. The geometric mean of the concentrations replaced missing concentrations, and the calculation of uncertainty for the concentrations greater than the MDL is based on the following equation 03

$$\text{Uncertainty} = \sqrt{(\text{error fraction} \times \text{concentration})^2 + (0.5 \times \text{MDL})^2} \quad \text{(Eqn. - 03)}$$

The error fraction is a user-provided estimation of the analytical uncertainty of the measured concentration or flux. For example, Xie et al. (2014) and Han et al. (2017) used an error fraction of 0.2-0.3 and 0.2 for organics, respectively. In this work, the error fraction was set to be 0.2 for all species. The detailed discussions of the determination and application of PMF are reported by Paatero et al. (2002) and Zhou et al. (2004).

3. Results and Discussion

3.1. Concentrations of Biogenic SOA Tracers

Figure 4 shows the temporal trends in the concentrations of BSOA tracers in the Chichijima samples (Figures 4a–4n), and Table 1 presents their annual and seasonal concentration ranges and average values, together with the standard deviations. The concentrations of BSOA tracers in the Chichijima aerosols ranged from 0.03–14.1 ng m^{-3} (avg. 2.35 ± 2.71 ng m^{-3}), which are lower than those reported for Okinawa Island (0.09-15.5 ng m^{-3}, avg. 4.53 ng m^{-3}) (Zhu et al., 2016) and the East China Sea (1.1-135 ng m^{-3}, 22.9 ng m^{-3}) (Kang et al., 2018). The East China Sea is closer to the Asian continent than the Okinawa and Chichijima Islands. The lower concentrations of BSOA tracers suggest that continental air masses influence is weakened over in remote Chichijima due to aerosol aging, dry/wet deposition during long-range atmospheric transport, and dilution of pristine air masses.

3.1.1. Isoprene-derived SOA Tracers

Isoprene (2-methyl-1,3-butadiene, C_5H_8) is a volatile unsaturated hydrocarbon that is mainly emitted from terrestrial vegetation, maritime phytoplankton, seaweed (Shaw et al., 2003) and microorganisms, including cyanobacteria. The production of isoprene is temperature-dependent (Sharkey and Singsaas, 1995; Kurihara et al., 2010; Li et al., 2011). Although the oceanic emissions of isoprene are much smaller than the terrestrial emissions, they significantly impact the atmospheric chemistry and cloud properties in the remote marine boundary layer because of the short lifetime (1–2 h) and high reactivity (Bonsang et al., 1992; Hackenberg et al., 2017). Hence, due to the short lifetime, isoprene cannot be transported long distances after the emission in source regions. Therefore, the isoprene-derived SOA (*i*SOA) tracers detected in the remote marine atmosphere are formed by the oxidation of the maritime-emitted isoprene or transported to the marine site from the adjacent continent after the formation of *i*SOA (Fu et al., 2016; Kang et al., 2018). Accordingly, the *i*SOA tracers abundant in winter and spring were mostly long-range transported from the Asian continent. In contrast, summertime higher *i*SOA tracers were formed by the oxidation of isoprene emitted in the remote marine atmosphere.

Six *i*SOA tracers including 2-MGA, three C_5-alkene triols, and two 2-MTLs were identified in the Chichijima aerosol samples (Figures 4b–4h). The total concentrations of the *i*SOA tracers varied from 0.007–3.98 ng m^{-3}, with a mean of 0.69 ± 0.67 ng m^{-3} (Table 1). The mean concentration of the *i*SOA tracers at Chichijima is comparable to those reported for the North Pacific to the Arctic (Ding et al., 2013) and the North Pacific (Fu et al., 2011), but much lower than those reported for the South and East China Sea (Ding et al., 2012; Kang et al., 2018).

We found 2-MTLs to be the dominant *i*SOA tracer in Chichijima aerosols. The concentrations of 2-MTL_2 were twice those of 2-MTL_1 with concentrations ranging from 0.005–2.07 ng m^{-3} (avg. 0.29 ± 0.33 ng m^{-3}) and 0.003–0.97 ng m^{-3} (0.14 ± 0.15 ng m^{-3}), respectively. The concentrations of 2-MTLs ranged from 0.007–3.04 ng m^{-3} (0.43 ± 0.47 ng m^{-3}), which are several times lower than those (0.05–7.22 ng m^{-3}, avg. 1.58 ± 1.50 ng m^{-3}) reported in the aerosols from Okinawa Island in the WNP (Zhu et al., 2016). 2-MGA is formed by the oxidation of methacrolein and methacrylic acids derived from isoprene (Surratt et al., 2006). The average concentration of 2-MGA was determined to be 0.15 ± 0.14 ng m^{-3} (0.005-0.79 ng m^{-3}). C_5-alkene triols are a photooxidation product of isoprene. Its concentrations were

detected in the range from 0.006–1.28 ng m^{-3}, with an average of 0.12 ± 0.16 ng m^{-3} in Chichijima aerosols.

3.1.2. Monoterpene-derived SOA Tracers

Four monoterpene-derived SOA tracers (*m*SOA tracers), including PNA, PA, 3-HGA, and 3-MBTCA were detected in the Chichijima aerosols (Figures 4i–4m). Monoterpenes are photooxidation products of α/β-pinene with O_3 and OH radicals, mainly emitted from the needle leaves of the higher plants and trees (Hoffmann et al., 1997; Glasius et al., 2000; Iinuma et al., 2004). These components have been utilized to estimate the role of monoterpene oxidation in SOA formation (Griffin et al., 1999). The concentrations of *m*SOA tracers in Chichijima samples ranged between 0.005 to 11.1 ng m^{-3}, with an average of 1.14 ± 1.93 ng m^{-3} (Table 1). This average concentration is higher than those reported from remote sites in the North Pacific and Indian Ocean (Fu et al., 2011), but lower than those reported from coastal sites in the South China (Ding et al., 2012) and East China Sea (Kang et al., 2018).

A very low level of first-generation products such as PNA (avg. 0.05 ± 0.08 ng m^{-3}) and PA (0.19 ± 0.28 ng m^{-3}), were detected in the Chichijima aerosols. The vapor pressure of PNA is higher than that of PA (Bhat and Fraser, 2007), so PNA is not as easily saturated in the atmosphere nor does it nucleate as readily as PA. Therefore, PNA is expected to have a smaller fraction in the aerosol phase than PA. 3-HGA was found to be the most abundant among the SOA tracers detected in the Chichijima aerosols. The concentration range of 3-HGA was 0.002–8.04 ng m^{-3} with an annual average of 0.71 ± 1.26 ng m^{-3}. Both 3-HGA and 3-MBTCA are novel *m*SOA tracers that have been reported to generate in α-pinene smog-chamber experiments under UV-radiation in the presence of NO_x (Claeys et al., 2007). In addition, PNA can be further photochemically oxidized to a higher-generation product 3-MBTCA in the presence of oxidants (Szmigielski et al., 2007).

Interestingly, we found a substantial amount of 3-MBTCA in Chichijima aerosols. The concentrations of 3-MBTCA ranged from 0.001–2.51 ng m^{-3}, with an average of 0.29 ± 0.49 ng m^{-3}. This 3-MBTCA concentration in Chichijima is lower than that reported at Okinawa Island, which is very close to the Asian continent (Zhu et al., 2016), but comparable to those reported in remote marine aerosols over the Pacific and Atlantic Oceans (Fu et al., 2011). The concentration of 3-MBTCA in the atmosphere has noted to be significantly enhanced by high levels of NO_x (Claeys et al., 2007), which is abundant at urban sites compared to remote marine sites. Kang et al. (2018) found higher concentrations of 3-MBTCA at a coastal site in

the East China Sea, which is highly influenced by the continental outflows of anthropogenic emissions. These findings indicate that the low concentration of 3-MBTCA in the western North Pacific is associated with the lesser impact of anthropogenic sources than the East China Sea. However, it is also evidence for the aging effect of 3-MBTCA during long-range transport from the continental source region to the remote site.

3.1.3. *β*-Caryophyllene-derived SOA Tracer

β-Caryophyllinic acid can rapidly form in the atmosphere by the ozonolysis or photooxidation of *β*-caryophyllene (Jaoui et al., 2007). With relatively low vapor pressure, *β*-caryophyllinic acid is highly reactive and thus is usually the least reported SOA component in atmospheric aerosols. Sesquiterpenes and isoprenoids are stored in plant tissues such as glands or resin ducts in the form of liquid micelles due to their lesser volatility (Fall, 1999). They play protective roles against pathogens and insects (Keeling and Bohlmann, 2006). BB (i.e., smoldering, charring, and flaming) may induce the emissions of different VOC classes including *β*-caryophyllene into the atmosphere (de Lillis et al., 2009). BB not only stimulates the emissions of sesquiterpene but also substantially impacts the formation yields of SOAs in the air (Mentel et al., 2013).

Interestingly, an abundant presence of the *β*-caryophyllene-derived SOA tracer (*β*-caryophyllinic acid or *c*SOA tracer) was detected in the Chichijima aerosols (Figure 4n). The concentrations of this *β*-caryophyllinic acid ranged range from 0.002–2.81 ng m^{-3}, with an average of 0.60 ± 0.72 ng m^{-3} (Table 1). This value is lower than those reported for the marine aerosols of Okinawa (Zhu et al., 2016) and the coastal aerosols of the East China Sea (Kang et al., 2018). This comparison further suggests that the continental emissions of *β*-caryophyllene profoundly influence the formation of *c*SOA in the marine atmosphere, which is discussed later in section 3.2.3.

3.2. Possible Sources and Factors Affecting the BSOA Tracers Over Chichijima Island

Our previous studies found that atmospheric circulations significantly affect the composition and seasonal variations of aerosol particles in the WNP (Verma et al., 2015; 2018). Moreover, meteorological conditions also play a significant role in producing BSOA tracers (Szmigielski et al., 2007). The chlorophyll-a is a good tracer of marine biological activities, which affects the production of marine BVOCs (Ooki et al., 2015). Boreddy et al. (2015) reported higher chlorophyll-a concentrations in winter and spring than in summer and autumn

in the WNP. However, the lower biological activities and, subsequently, lesser VOC emissions might not be so significant for the SOA emissions over the WNP region. Moreover, the photochemical processing of BVOCs, followed by their atmospheric circulation over the WNP and gas-to-particle conversion of BVOCs via atmospheric oxidation, may another important factor controlling the seasonal variations of BSOA tracers, which follow changes in the ambient temperature and precipitation.

Supplementary Figures S3a and S3b show the temporal trends and monthly mean variation of the NO_3^- concentrations in the Chichijima aerosols from 2010 to 2012. The seasonal distributions of NO_3^- showed higher concentrations in winter and spring, while they are lower in summer and autumn. Similar temporal and seasonal variations were found between NO_3^- concentrations and high-NO_x SOA tracers (2-MGA, 3-HGA, and 3-MBTCA). In contrast, trends were opposite for low-NO_x SOA tracers (2-MTLs, C_5-alkene triols) in the Chichijima aerosols (Figures 4b–4m and 5b–5m), which indicates a possible role of NO_3 radicals in the formation and seasonal variations of SOA tracers in the Chichijima aerosols. Kang et al. (2018) reported a correlation between NO_3^- and high-NO_x *i*SOA tracers and *m*SOA tracers. They suggested that this kind of relationship indicates the influence of NO_3 in the formation of high-NO_x *i*SOA tracers and *m*SOA traces in the marine aerosol samples. Therefore, the abundance and seasonal variations of BSOA tracers in the Chichijima aerosols might be significantly affected by several parameters, i.e., long-range transported anthropogenic and pristine air masses, NO_3 radicals, and chlorophyll-a concentrations, which we discuss in the next section.

3.3. Seasonal Variations of SOA Tracers

Table 1 shows a summary of the seasonal concentrations of SOA tracers in the Chichijima aerosols. The overall concentrations of SOA tracers were found to be higher in winter (avg. 3.40 ± 2.18 ng m^{-3}) and spring (avg. 3.35 ± 3.83 ng m^{-3}) than summer (1.05 ± 1.12 ng m^{-3}) and autumn (1.68 ± 2.17 ng m^{-3}). The monthly variations of biogenic SOA tracer concentrations were at their maximum in spring, followed by autumn (Figure 5a). SOA tracers are highly water-soluble because they contain multiple hydroxy and carboxyl groups, and therefore they can be easily scavenged by precipitation and act as CCN. In Chichijima, significant rainfall occurs in early summer (June) to mid-autumn (October) (Figure 2), which would lead to the scavenging of SOA tracers in summer/autumn by the occasional rain events in Chichijima and its surrounding areas.

3.3.1. Seasonal Variations of Isoprene-derived SOA Tracers

The *i*SOA tracers concentrations in the Chichijima aerosols exhibited no significant seasonal variation (Figure 5b). Their average concentrations are comparable over the four seasons i.e. winter (avg. 0.78 ± 0.56 ng m^{-3}), summer (0.73 ± 0.90 ng m^{-3}), spring (0.71 ± 0.52 ng m^{-3}), and autumn (0.56 ± 0.67 ng m^{-3}) (Table 1). This insignificant seasonal variation suggests that although the contribution of *i*SOA tracers to organic aerosols (OA) is significant in the Chichijima, their production seems to occur almost irrespective of their source regions, except for 2-MGA, which shows a clear winter maximum. Surratt et al. (2006) noted that total concentrations of *i*SOA tracers are affected by the emission and reaction rates of BVOCs under different meteorological conditions such as the ambient temperature and RH. The atmospheric levels of NO_x significantly influence the production of *i*SOA tracers (Ding et al., 2014). A significant amount of *i*SOA tracers in winter suggest that enhanced long-range atmospheric transport of pollutants such as NO_x controls the production of *i*SOA tracers over the remote island.

2-MTLs are formed by the photooxidation of isoprene initiated by OH radicals, which was observed first time in the aerosols collected from the Amazonian rain forest (Claeys et al., 2004). Based on laboratory experiments, Zhang et al. (2011) proposed that the production of 2-MTLs is enhanced under low-NO_x and high RH conditions. Apparently, the remote marine atmosphere is characterized by low-NO_x with high-RH, supporting the formation of MTLs instead of 2-MGA. The insignificant correlation of 2-MTLs with NO_3^- (r = 0.03) also suggests their formation in the low-NO_x condition. We observed insignificant seasonal variations of 2-MTLs in the Chichijima aerosols. The monthly mean concentrations of 2-MTLs were elevated from June to August (Figures 5c and 5d). The seasonally averaged concentrations of 2-MTLs were 0.58 ± 0.73 ng m^{-3} in summer, 0.41 ± 0.30 ng m^{-3} in winter, 0.38 ± 0.30 ng m^{-3} in spring, and 0.37 ± 0.42 ng m^{-3} in autumn (Table 1). The predominance of 2-MTLs among *i*SOA tracers was also reported for the Okinawa aerosols together with higher loadings in summer (Zhu et al., 2016). The long-range atmospheric transport of anthropogenic pollutants (e.g., NO_x) may contribute to a decline in the production of low-NO_x *i*SOA tracers (2-MTLs) during winter and spring over Chichijima Island.

The isoprene emission rates might be much higher in summer than in spring, autumn and winter due to the change of leafage, temperature, and light. These factors also affect the isoprene reactions, causing a higher production of 2-MTLs in the summer season (Xia and

Hopke et al., 2006). The summertime maximum of 2-MTLs is probably associated with the enhanced emission of isoprene from terrestrial and marine biota, followed by its atmospheric oxidation. This occurs because isoprene emissions can increase by a factor of 10 with a 10 °C increase in the leaf temperature (Sharkey and Singsaas, 1995; Rasulov et al., 2010; Li et al., 2011). Moreover, phytoplankton and marine biota are unique sources for isoprene emissions in the remote marine atmosphere (Bonsang et al., 1992; Broadgate et al., 1997). If the *i*SOA tracers were formed over the marine atmosphere, the seasonal and spatial distribution of 2-MTLs could be assumed to correlate with the mass of phytoplankton in the marine site. The trade winds from the central Pacific to Chichijima might transport the isoprene emitted from marine biota in summer (Figure 3). In addition, summertime low-NO_x and high RH conditions may enhance the production of 2-MTLs in a pristine environment over the WNP (Zhang et al., 2011). It also suggests that the formation of 2-MTLs was highly influenced by the local emissions and meteorological conditions in the pristine environment of the WNP (Ding et al., 2013).

The insignificant correlations of 2-MTLs with BB tracer (levoglucosan) during winter ($r = 0.04$, $n = 37$) and spring ($r = 0.26$, $n = 40$) (Figures 6a and 6b) imply that the isoprene emissions from BB are negligible. The higher levels of 2-MTLs from January to March may be associated with the isoprene emissions from marine phytoplankton. A high level of chlorophyll-a was observed near Chichijima Island from January to March, which is in good agreement with the wintertime isoprene oxidations into 2-MTLs in the marine atmosphere over Chichijima and its surrounding areas. 2-MTLs are the acid-catalyzed hydrolysis products of isoprene epoxydiols (IEPOX) in the aerosol aqueous-phase (Riva et al., 2016). Chichijima Island is highly influenced by anthropogenic aerosols from East Asia in winter and spring, with higher levels of SO_4^{2-} and NO_3^- (Boreddy et al., 2015), which likely increase the acidity of aerosols and the formation of 2-MTLs.

In a chamber experiment, Surratt et al. (2006) reported the formation of 2-MGA by the photooxidation of isoprene under high-NO_x conditions. 2-MGA is an oxidation product of methacrolein and methacrylic acid, which are formed by the gas-phase oxidation of isoprene at high-NO_x levels (Claeys et al., 2004). We found that 2-MGA is the second most abundant *i*SOA tracer at Chichijima with different seasonal patterns than low-NO_x products (i.e., 2MTLs). Its concentration was higher in winter (avg. 0.22 ± 0.15 ng m^{-3}) followed by spring (0.19 ± 0.16 ng m^{-3}) and lower in summer (0.07 ± 0.08 ng m^{-3}). 2-MGA is most abundant in mid-winter (January), to early spring (March) (Figure 5e). Surratt et al. (2006) and Zhang et al.

(2011) reported an enhancement of 2-MGA in low RH conditions. The wintertime maximum of 2-MGA at Chichijima may be associated with the wintertime low RH and high-NO_x conditions via the long-range transport of pollutants from East Asia. The lowest concentrations of 2-MGA in June may be partly associated with its washout by rain at Chichijima and its surroundings (Figure 2).

*i*SOA tracers were comprised of effectively nonvolatile material that could be allowed *i*SOA to be long-lived in the atmosphere (Lopez-Hilfiker et al., 2016). In a NO_3 initiation experiment, Hoyle et al. (2011) reported a significant yield of *m*SOA and *i*SOA tracers by the reaction of isoprene and monoterpene with nitrate radical (NO_3), a nighttime product of NO_2 and O_3. Kang et al. (2018) also found the correlation of high-NO_x *i*SOA tracers (2-MGA and C_5-alkene triols) with NO_3^- and suggested the close connections between the formation of SOA tracers and NO_3 in marine aerosols. Although 2-MGA, a high-NO_x *i*SOA tracer, showed seasonal variation similar to NO_3^- we did not find significant correlations of 2-MGA with NO_3^- ($r = 0.55$). This suggests that 2-MGA likely formed at upwind in the Asian continental region and subsequently transported to the Chichijima Island in the WNP. The SOA tracers were transported to long distances, but its impact gradually decreased because of the dilution and deposition effects during long-range atmospheric transport.

The diagnostic mass concentration ratios of *i*SOA tracers can provide valuable information about their sources and formation processes as well as their photochemical aging and the impact of long-range transported anthropogenic aerosols on *i*SOA formation. We determined the ratio of low-NO_x products (2-MTLs) to the high-NO_x product (2-MGA) to understand the biogenic emissions of *i*SOA tracers and the influence of NO_x and local meteorological conditions on their formation (Lewandowski et al., 2013). The average seasonal ratio of 2-MTLs/2-MGA shows a maximum in summer (5.22) and autumn (4.12) and a minimum in winter (2.02) and spring (2.80) (Table 2). A significantly high annual average of 2-MTLs/2-MGA ratio (3.43) in Chichijima aerosols suggest a decrease in the concentration of 2-MGA due to a dilution effect during long-range transport from the continental region to Chichijima Island. The lower ratios in winter and spring are in good agreement with the enhanced levels of NO_x in these seasons.

C_5-alkene triols are mainly formed by the reactive uptake of the isoprene epoxydiols (IEPOX) produced by the reaction of isoprene with OH and HO_2 radicals in low-NO_x conditions. The insignificant seasonal variation of C_5-alkene triols indicates the importance of

526 regional or local sources during the sampling campaign. C_5-alkene triols and 2-MTLs show
527 excellent linearity and a significant correlation coefficient in all seasons (Figures 7a–7d). These
528 results suggest that C_5-alkene triols and 2-MTLs are derived from the same sources via an
529 identical formation mechanism. In addition, the insignificant correlations of C_5-alkene triols
530 and NO_3^- (r = 0.20), indicates their formation by isoprene photooxidation in the low-NO_x
531 environment of the western North Pacific. The monthly mean concentrations of C_5-alkene
532 triols showed a prominent peak in mid-winter (January) to early spring (March) (Figures 5f–
533 5h), which are in good agreement with the higher chlorophyll-a concentrations during similar
534 periods, suggesting that the significant isoprene emissions from the oceanic phytoplankton in
535 the marine atmosphere of the WNP .

536 The concentration ratio of C_5-alkene triols (low-NO_x) and 2-MTLs (high RH) can be
537 used to understand the influence of anthropogenic emissions on the formation of BSOA tracers.
538 The C_5-alkene triols/2-MTLs ratio was reported to be <0.1 in aerosol samples collected over
539 the remote ocean, whereas ratio >0.6 was reported over the coastal ocean (Fu et al., 2011). The
540 seasonal mean C_5-alkene triols/2-MTLs ratios in the Chichijima samples were higher in spring
541 (0.37) and winter (0.34) than in summer (0.15) and autumn (0.22) (Table 2). The lower ratios
542 in summer and autumn are in good agreement with a laboratory experiment of Kleindienst et al.
543 (2009), in which a lower ratio was obtained for the photooxidation of isoprene in the absence
544 of NO_x. Furthermore, C_5-alkene triols can be transformed into 2-MTLs through acid-catalyzed
545 hydrolysis in summer and autumn seasons suggested the intra-transformation of *i*SOA tracers
546 under suitable atmospheric conditions.
547

548 **3.3.2. Seasonal Variations of Monoterpene-derived SOA Tracers**

549 The monoterpene-derived SOA (*m*SOA) tracers in the Chichijima aerosols presented
550 the highest concentration in spring (avg. 1.96 ± 2.96 ng m^{-3}) followed by winter (1.45 ± 1.42
551 ng m^{-3}), autumn (0.83 ± 1.39 ng m^{-3}), and summer (0.20 ± 0.39 ng m^{-3}) (Table 1 and Figure
552 5i). The first-generation monoterpene product (PA) showed a clear seasonal trend with higher
553 levels in winter and spring, whereas low levels were observed in summer and autumn. The
554 PNA showed a similar seasonality with low concentrations (Figures 5j and 5k). Bud formation
555 and elongation are maximized in spring, along with the emission rates of terpenes (Kim, 2001).
556 3-HGA and 3-MBTCA were found to be the dominant *m*SOA tracers detected in the
557 Chichijima aerosols, and thus their seasonal variations significantly affect the seasonal trends
558 of those *m*SOA tracers. 3-HGA showed a high level in spring (avg. 1.31 ± 2.0 ng m^{-3})

559 followed by winter (0.86 ± 0.90 ng m^{-3}), whereas 3-MBTCA is equally distributed in winter
560 (0.32 ± 0.36 ng m^{-3}), spring (0.40 ± 0.69 ng m^{-3}), and autumn (0.31 ± 0.57 ng m^{-3}) (Table 1
561 and Figures 5l and 5m). A high-NO_x level in spring may enhance the formation of 3-HGA and
562 3-MBTCA (Surratt et al., 2006). 3-HGA and 3-MBTCA show good correlations in each season,
563 which suggests that the formation mechanisms of both *m*SOA tracers in the WNP are similar
564 (Figures 7e–7h).

565 In addition, the monthly mean concentrations of 3-HGA and NO_3^- were found to
566 increase from late autumn (November) and peaked in early spring (May), which prolonged up
567 to mid-spring (March). The concentrations started to decrease from early summer (May) to
568 mid-autumn (October). In the preceding periods, emissions of anthropogenic gases (NO_x and
569 SO_x) are usually high in the East Asian countries, which might initiate the oxidation of
570 monoterpenes and isoprene followed by subsequent formation of *m*SOA tracers (3-HGA and 3-
571 MBTCA) and *i*SOA tracers (2-MGA), respectively. Although the seasonal trends of 3-HGA
572 and NO_3^- are similar in the Chichijima aerosols, the negative correlation of NO_3^- with 3-HGA (r
573 = −0.20) and 3-MBTCA (r = −0.09) suggest that both *m*SOA tracers might be formed in the
574 continental region and transported to the downwind region in the WNP during winter and
575 spring (Figures 7i and 7j). The previous study also reported a long-range transport of *m*SOA
576 tracers from the East Asian continent to the remote marine region (Kang et al., 2018).

577 The lower levels of 3-HGA and 3-MBTCA in summer may be associated with
578 summertime lower emissions of monoterpenes, which decline the formation of *m*SOA tracers
579 over the remote Chichijima Island. The meteorological parameters may significantly influence
580 the formation of *m*SOA tracers in the WNP. We note that the seasonal concentration of 3-HGA
581 is slightly different from that of 3-MBTCA, suggesting an additional formation process for 3-
582 MBTCA via the photochemical oxidation of PNA in the presence of oxidants (Szmigielski et
583 al., 2007). The significant level of 3-MBTCA and low concentrations of PNA in the
584 Chichijima aerosols might indicate aerosol aging during long-range atmospheric transport.

585 3-MBTCA is an oxidation product of PNA and PA (Claeys et al., 2007). Therefore, the
586 3-MBTCA/(PNA+PA) ratios can be used to better understand the aging of *m*SOA tracers in the
587 atmosphere (Kulmala et al., 2011). Ratios greater than unity indicate the photochemical aging
588 of SOA, whereas ratios <1 indicate relatively fresh SOA. The average 3-MBTCA/(PNA+PA)
589 ratios in the Chichijima aerosols were 1.26, 1.37, 1.13, and 1.40 in winter, spring, summer, and
590 autumn, respectively (Table 2). According to the results, we hypothesized the possibilities of

591 the aging effect in the Chichijima aerosol during long-range atmospheric transport. However,
592 further research is needed to better evaluate the photochemical formation or aging of aerosol
593 during long-range transport from Asian continent to the WNP.

594 **3.3.3. Seasonal Variation of *β*-Caryophyllene-derived SOA Tracer**

595 The *c*SOA tracer showed a clear winter maximum that is differed from those of the
596 *i*SOA and *m*SOA tracers (Figures 5b, 5i and 5n). The *c*SOA tracer exhibited the highest
597 concentration in winter (avg. 1.23 ± 0.68 ng m^{-3}) followed by spring (0.66 ± 0.73 ng m^{-3}),
598 autumn (0.37 ± 0.61 ng m^{-3}), and summer (0.12 ± 0.21 ng m^{-3}) (Table 1). Sesquiterpenes,
599 including *β*-caryophyllene, can accumulate in plant leaves and be emitted to the atmosphere.
600 However their global emission (36 Tg C yr^{-1}) is less than those of isoprene (634 Tg C yr^{-1}) and
601 monoterpenes (89 Tg C yr^{-1}) (Acosta Navarro et al., 2014). They can evaporate and emit into
602 the atmosphere substantially via the BB of higher plants (Ciccioli et al., 2014; Sekimoto et al.,
603 2018).

604 The *c*SOA tracer concentrations in Chichijima aerosols (avg. 0.60 ± 0.72 ng m^{-3}) are
605 notably lower than those reported for coastal site and Marine Island in the WNP, which are
606 significantly influenced by continental outflows from East Asia. Kang et al. (2018) reported
607 high levels of the *c*SOA tracer (2.9 ng m^{-3}) in the coastal East China Sea, strongly influenced
608 by BB aerosols in winter. Zhu et al. (2016) also reported relatively high concentrations of the
609 *c*SOA tracer (1.63 ng m^{-3} in winter and 0.82 ng m^{-3} in spring) at Okinawa Island, located in
610 the east of the East China Sea and is influenced by westerly winds from the Asian continent.
611 The comparisons of *c*SOA tracer of Chichijima with those from the East China Sea and
612 Okinawa Island reveal that the significant decline in the *c*SOA tracer concentrations in the
613 Chichijima aerosols is largely caused by dry/wet scavenging along the atmospheric transport
614 pathway over the WNP.

615 As seen in Figure 4n, the concentrations of *β*-caryophyllinic acid substantially increase
616 from 2010 to 2012. Monthly composite images of the Moderate Resolution Imaging
617 Spectroradiometer (MODIS) active fire spots were obtained to identify the geographically
618 active fire areas as possible source regions of BB tracers (https://earthdata.nasa.gov/data/near-
619 real-time-data/firms/). Three years of monthly MODIS active fire spot detections in Siberia,
620 East Asia, and Southeast Asia indicate a significant increase of fire activity in mid-autumn to
621 late spring (Figure S4). The BB for cooking and space heating is common in the East Asian

622 countries during the cold seasons (mid-autumn to mid-spring), which might be a significant
623 source to the downwind regions. Interestingly, concentrations of levoglucosan and *β*-
624 caryophyllinic acid also increased during mid-autumn to mid-spring, suggesting that *c*SOA
625 tracer is strongly associated with BB in East Asia (Figure 8). The BB activities in the Asian
626 continent significantly impact on the concentration of *c*SOA tracers in the remote marine
627 atmosphere over the WNP during the mid-autumn to mid-spring. Air mass trajectories also
628 support the transport of air parcels from East Asia, Siberia, and Russian Far East over
629 Chichijima Island (Figure 3).

630 The concentration ratios of the *i*SOA/*c*SOA tracers in the Chichijima aerosols are much
631 higher in summer (avg. 14.6) and autumn (9.64) than in spring (4.17) and winter (0.85) (Table
632 2). This indicates the enhanced emissions of isoprene and subsequent formation of *i*SOA
633 tracers in warmer seasons and the enhanced emission of *β*-caryophyllene in colder seasons by
634 BB in East Asia followed by atmospheric transport and oxidation over the WNP. The isoprene
635 emissions are known to increase with an increase in ambient temperature in summer and
636 autumn (Ding et al., 2014). In Chichijima, higher concentrations of *i*SOA tracers were recorded
637 during the warmer periods when biogenic emissions increase due to the higher temperatures.
638 These results also indicate a significant contribution of *i*SOA tracers from local vegetation and
639 marine phytoplankton in the Pacific. The winter minima of *i*SOA/*c*SOA ratios are amplified by
640 a greater contribution of *c*SOA tracer associated with BB in East Asia.

641 **3.4. Contributions of Oxidation Products of BVOCs to Organic Carbon (OC)**

642 In this study, we applied a tracer-based method proposed by Kleindienst et al. (2007) to
643 roughly estimate the loading of biogenic secondary organic carbon (SOC) using the SOA tracer
644 concentrations measured in the Chichijima aerosols and the mass fractions (f_{SOC}) of laboratory-
645 derived tracers: 0.155 ± 0.039 for isoprene, 0.231 ± 0.111 for monoterpene, and 0.0230 ±
646 0.0046 for *β*-caryophyllene. The SOC concentrations derived from each type of precursor were
647 calculated using the following equation: $f_{SOA} = \Sigma_i[tri]/[SOA]$, where [tri] is concentrations of
648 tracer, i, in ng m^{-3} and [SOA] is the mass concentrations of SOA. We note that the tracer-
649 based method simplifies the truly complex system of the real atmosphere (Stone et al., 2010).
650 Kleindienst et al. (2007) applied the total of 3 and 9 tracers to derive f_{SOC} of isoprene and α-
651 pinene, respectively. In contrast, we detected six compounds (i.e., 2-MGA, three C_5-alkene
652 triols, and two diastereoisomeric 2-MTLs) derived from isoprene and four compounds (i.e., 3-
653 HGA, PNA, PA, and 3-MBTCA) from monoterpene, whose concentrations were used to

estimate the f_{SOC} derived from the precursors.

We consider that the uncertainties associated with the differences between the tracers used for the SOC estimation to be within the range of those of the tracer-based approach itself (25%, 48% and 22% for isoprene-, monoterpene-, and β-caryophyllene-derived SOA, respectively), based on the standard deviation in the f_{SOC} mentioned above. Although the estimation of biogenic SOC is associated with some uncertainty due to the difference in the number of SOA tracers used for calculation, this is a widely accepted approach for estimating the SOC in atmospheric aerosols (Lewandowski et al., 2013). Kleindienst et al. (2009) reported that the f_{SOC} derived for isoprene (range 0.117–0.231, ave. 0.156) in the absence of NO_x is similar to that obtained under high-NO_x (0.11–0.65 ppm) conditions, although the NO_x influence of the f_{SOC} for other VOCs is not clear. Hence, we emphasize that this tracer-based method is highly applicable to the present study.

Table 3 shows the seasonal concentrations of the total SOC and their contributions to OC concentrations in the Chichijima aerosols. These OC data are available in Boreddy et al. (2018). The total SOC concentrations ranged from 0.11–174 ngC m^{-3} (avg. 34.8 ± 38.2 ngC m^{-3}), which accounts for 0.02–32.0% (6.11 ± 6.42%) of the OC in the Chichijima samples. These levels are comparable to those (0.25–157 ngC m^{-3}, 35.8 ngC m^{-3}) reported for the Okinawa aerosols (Zhu et al., 2016). We found the highest average concentration of biogenic SOC (64.6 ± 34.5 ngC m^{-3}) and contribution to OC (12.4 ± 6.95%) in winter, followed by spring (41.3 ± 42.6 ngC m^{-3}, 5.48 ± 5.41%), autumn (17.3 ± 25.8 ngC m^{-3}, 3.17 ± 3.83%), and summer (10.7 ± 12.5 ngC m^{-3}, 2.67 ± 2.98%). More oxidants (NO_x, O_3, and SO_2) are likely transported over the WNP from the Asian continent due to the strong westerly winds in winter (Figure 3), resulting in more SOAs from VOC precursors. Therefore, higher biogenic SOC concentrations and their higher contributions to OC are reasonable in the winter season.

The average concentrations of isoprene-derived SOC (*i*SOC) were found to be almost equally distributed in winter (avg. 5.00 ± 3.60 ngC m^{-3}), summer (4.70 ± 5.77 ngC m^{-3}), and spring (4.52 ± 3.33 ngC m^{-3}), with slightly lower concentration observed in autumn (3.49 ± 4.48 ngC m^{-3}). These *i*SOC levels in Chichijima are comparable to those reported for marine aerosols over Okinawa Island (3.86 ± 3.86 ngC m^{-3}) (Zhu et al., 2016), which are significantly lower than those from the East China Sea (39.8 ± 55.4 ngC m^{-3}) (Kang et al., 2018). The average contribution of *i*SOC to OC in the Chichijima aerosols was maximum in summer (1.16 ± 1.24%), followed by winter (1.02 ± 0.95%). Interestingly, the highest contribution of *i*SOC

686 to total SOC concentration was observed in summer (45.0 ± 24.9%), followed by autumn (35.5
687 ± 21.5%) (Table 3). This result indicates that significant amounts of isoprene are emitted from
688 terrestrial vegetation and marine phytoplankton and oxidized to SOC over the WNP under
689 higher ambient temperatures and solar radiation during the warmer seasons (Goldstein et al.,
690 2007).

691 The seasonal mean concentration of monoterpene-derived SOC (*m*SOC) in the
692 Chichijima aerosols was found to be higher in spring (avg. 8.53 ± 12.9 ngC m^{-3}) and winter
693 (6.30 ± 6.15 ngC m^{-3}) than in autumn (2.49 ± 4.30 ngC m^{-3}) and summer (0.86 ± 1.69 ngC
694 m^{-3}) (Table 3). These concentration levels are much lower than those reported for coastal
695 aerosols over the East China Sea (50.2 ± 72.0 ngC m^{-3}) (Kang et al*.,* 2018). Although the
696 *m*SOC concentrations at Chichijima were found to be several times lower than those at
697 Okinawa (5.57 ± 4.74 ngC m^{-3}) (Zhu et al., 2016), the seasonal trends are very similar in both
698 islands. The westerly winds influence the atmospheric aerosols over the Okinawa and
699 Chichijima Islands because both are situated on the transport pathways of continental aerosols
700 and their precursors from the Asian continent. Thus, we hypothesized that the SOC
701 contribution in Chichijima was significantly affected by the monoterpene emissions and *m*SOA
702 tracers formation in the upwind continental regions.

703 We found *β*-caryophyllene-derived SOC (*c*SOC) to be a significant contributor to the
704 total BSOC in the Chichijima aerosols. *β*-Caryophyllinic acid is the photooxidation product of
705 *β*-caryophyllene, which has an endocyclic C=C bond. Because *β*-caryophyllene ($C_{15}H_{24}$)
706 contains more carbon atoms than isoprene (C_5H_8) and monoterpene ($C_{10}H_{16}$), the oxidation
707 products of *β*-caryophyllene generally have less vapor pressure than those of isoprene and
708 monoterpenes. Consequently, the differences in the formation processes of SOA and the
709 emission strength of their precursors, and the gas-to-particle conversion of different BVOCs
710 may be a potential factor in controlling the levels of *c*SOC in the Chichijima aerosols. The
711 seasonal mean concentration of *c*SOC was found to be highest in winter (53.6 ± 29.6 ngC m^{-3}),
712 followed by spring (28.6 ± 31.6 ngC m^{-3}), autumn (11.4 ± 20.3 ngC m^{-3}), and summer (5.20 ±
713 9.33 ngC m^{-3}) (Table 3). Interestingly, these *c*SOC concentrations are much higher than *i*SOC
714 and *m*SOCs throughout the study period.

715 The higher *c*SOC concentration in winter indicates an enhanced contribution of *β*-
716 caryophyllinic acid, which is associated with BB in the Asian continent. We note that westerly
717 winds can deliver significant amounts of BB-derived OA from the Asian continent to the WNP

718 (Verma et al., 2015). A similar seasonal trend (Figure 8) and the significant correlation
719 (Figures 6c–6g) of *c*SOA tracer with levoglucosan demonstrate that BB in East Asia likely
720 contributes significantly to *c*SOC in Chichijima aerosols. BB-derived OC (BB-OC) was found
721 to be highest in winter (0.97 ± 0.76 ngC m^{-3}), followed by spring (0.39 ± 0.51 ngC m^{-3}),
722 autumn (0.16 ± 0.29 ngC m^{-3}), and summer (0.08 ± 0.14 ngC m^{-3}) (Table 3). BB is considered
723 to affect the concentration levels of *c*SOA tracer and *c*SOC because the seasonal trend of BB-
724 OC (calculated from levoglucosan) was similar to that of *c*SOC. The above considerations
725 emphasize the contribution of SOC from BB and the production of *β*-caryophyllinic acid in the
726 continental region, followed by the atmospheric transports to the WNP.
727
728 **3.5. Sources Apportioned of SOA Tracers by PMF Analysis**

729 PMF is a powerful statistical tool for resolving the potential sources contributing to
730 atmospheric particles (Paatero and Tapper, 1994). PMF analysis was performed for
731 quantitative estimation of sources for the collected samples using tracer compounds for *i*SOA,
732 *m*SOA and *c*SOA. Based on a given understanding of sources of SOA tracers, 3 to 5 sources
733 were examined and total three interpretable factors were characterized by the enrichment of
734 each tracer compound, which reproduced more than 95% of SOA tracers. These factors were
735 selected on a basis of minimum robust and true Q values (goodness of fit parameters). The
736 PMF analysis results showed a good correlation between the predicted and observed
737 concentrations of SOA tracers and levoglucosan, which supported the excellent rationality of
738 the source apportionment (Figure S5). We also included the levoglucosan in the Chichijima
739 SOA tracer data sets in the PMF analysis to better understand the possible sources and
740 contributions of anthropogenic activities to the formation of BSOA tracers. Figure 9 shows the
741 factor profiles resolved by the PMF analysis of biogenic SOA tracers detected in the
742 Chichijima aerosols. Based on a PMF analysis of BB tracer (levoglucosan) and biogenic SOA
743 tracers, we detected three biogenic sources. Interestingly, we found that some factors represent
744 a combined influence of biogenic and BB sources as discussed below.

745 The first factor is characterized by *β*-caryophyllinic acid (95.4%) and levoglucosan
746 (92.9%) followed by 2-MGA (14.8%), C_5-alkene triols (11.9%), and 2-MTLs (7.35%). The
747 higher values of *β*-caryophyllinic acid and levoglucosan in factor 1 suggest the substantial
748 influence of BB on the production of *β*-caryophyllinic acid. Although *i*SOA tracers such as 2-
749 MGA, C_5-alkene triols, and 2-MTLs were detected as minor contributors to factor 1, they are
750 characterized as major contributors in factor 3. Due to the higher abundances of levoglucosan

751 and *β*-caryophyllinic acid, we conclude that factor 1 is influenced by *β*-caryophyllene
752 emissions and BB (Figure 9a). Here, we propose a hypothesis that *β*-caryophyllene is largely
753 emitted from plant tissues by evaporation during BB events in East Asia and oxidized in the
754 atmosphere during long-range transport of air masses to the remote Pacific Ocean.

755 Four *m*SOA tracers, including 3-MBTCA, PNA, PA, and 3-HGA, were found to have
756 contributed 96.8%, 96.6%, 88.5%, and 87.5%, respectively to factor 2. Due to the higher scores
757 of this factor, we conclude that factor 2 is characterized by monoterpene emissions from
758 terrestrial higher plants (Figure 9b). In factor 3, C_5-alkene triols, 2-MTLs, and 2-MGA
759 contributed 82.8%, 81.5%, and 76.1%, respectively. Hence, factor 3 is dominated by biogenic
760 isoprene oxidation products (Figure 9c). Overall, the average contributions of each factor to the
761 measured BSOA tracer concentrations were estimated by PMF analyses (Figure 10), where
762 *m*SOA tracers accounted for 44%, followed by *i*SOA tracers (29.6%) in the Chichijima
763 aerosols. The contribution of the *c*SOA and BB tracers accounts for 26.3% of the total SOA
764 tracer concentration. Levoglucosan and *β*-caryophyllinic acid in factor 1 indicate the
765 involvement of biogenic and BB sources. The PMF results show that biogenic emission
766 sources significantly contributed to the formation of BSOA tracers but were largely
767 superimposed by BB during the emissions of *β*-caryophyllene and the subsequent formation of
768 *c*SOA tracer.
769
770 **4. Summary and Conclusions**

771 In this study, atmospheric concentrations, seasonal distributions, and source
772 apportionments of biogenic isoprene, monoterpene, and sesquiterpene SOA tracers were
773 studied in aerosol samples collected at remote Chichijima Island in the western North Pacific.
774 The predominance of *m*SOA tracers, followed by *i*SOA and *c*SOA tracers were found in
775 Chichijima aerosol. The seasonal distributions of SOA tracers in Chichijima Island were
776 characterized by higher concentrations in winter and spring, and lower concentrations in
777 summer and autumn. *i*SOA tracers were formed with isoprene emissions from phytoplankton
778 in the Pacific region. In contrast, *m*SOA tracers were formed by the oxidation of monoterpenes
779 emitted at the continental region, consequently transported to Chichijima Island. The
780 contributions of *β*-caryophyllene oxidation products and BB-derived OC were dominant in
781 winter and spring due to long-range transport of continentally derived BB aerosols. The high-
782 NO_x BSOA tracers (2-MGA, 3-HGA, and 3-MBTCA) were aged and influenced by the long-

range transport of anthropogenic air masses. In contrast, the low-NO_x BSOA tracers (2-MTLs and C_5-alkene triols) were mostly produced by the oxidation of locally emitted isoprene.

The biogenic emissions of *β*-caryophyllene contributed to more formation of secondary organic carbon, followed by monoterpene and isoprene. A higher ratio of 2-MTLs/2-MGA resulted in the formation of *i*SOA tracers by isoprene emissions from marine phytoplankton. In contrast, the high 3-MBTCA/(PA+PNA) ratio indicated the aging of aerosols during long-range transport from the Asian continent. The meteorological parameters such as RH, temperature, and precipitation also influence the formation of biogenic SOA tracers over Chichijima. PMF analysis illustrates that monoterpene oxidation products could be the major sources for BSOA, followed by isoprene and *β*-caryophyllene in Chichijima aerosols over the WNP. This study demonstrates that the biogenic and anthropogenic emissions from the continental region significantly impact the formation and chemistry of BSOA over the WNP. Because previous model studies have not considered the emission of *c*SOA by BB, it is important to estimate how BB impacts the secondary formation of OA from the low volatility terpenoids accumulated in terrestrial vegetation at regional and global scales, which are easily emitted to the air on biomass burning.

The oxidation of isoprene emitted from phytoplankton could significantly influence the cloud droplet number and affect marine cloud condensation nuclei (CCN) in the remote marine atmosphere. In addition, the oxidation process of maritime BVOCs is significantly influenced by the long-range transport from the continent. The SOA tracers are highly water-soluble due to –OH and –COOH groups. Therefore, the chemical and physical properties of cloud condensation nuclei (CCN) and gas to particle conversion could be elucidated by the atmospheric compositions and seasonal studies of SOA tracers in the remote marine atmosphere.

Data Availability Statement

The data set of processed absorption coefficients is available at https://data.mendeley.com/datasets/jnfsk4xbvr/1.

Acknowledgments

We acknowledge the financial support from the Japan Society for the Promotion of Science (JSPS) through grant-in-aid Nos. 19204055 and 24221001. The authors declare no

competing financial interests. The meteorological data was obtained from the Japan Meteorological Agency (https://www.jma.go.jp/jma/indexe.html). The authors are grateful to the NOAA Air Resources Laboratory (ARL) for the provision of the HYSPLIT transport and dispersion model (http://www.ready.noaa.gov). Nitrate (NO_3^-) and organic carbon (OC) data is available through Boreddy et al., 2015 and Boreddy et al., 2018, respectively. We gratefully acknowledge the MODIS for the monthly detection of MODIS active fire/hot spots from Terra and Aqua satellites by EOSDIS from 2010 to 2012 periods (https://earthdata.nasa.gov/data/near-real-time-data/firms/). We appreciate the constructive comments and suggestions of the Editors and two anonymous reviewers. The authors would like to thank Enago (www.enago.jp) for the English language review.

825 **References**

826 Acosta Navarro, J. C., Smolander, S., Struthers, H., Zorita, E., Ekman, A. M. L., Kaplan, J. O.,
827 Guenther, A., Arneth, A., & Riipinen, I. (2014). Global emissions of terpenoid VOCs from
828 terrestrial vegetation in the last millennium. *Journal of Geophysical Research: Atmosphere*,
829 *119*, 6867–6885. https://doi:org/10.1002/2013JD021238

830 Bhat, S., & Fraser, M. P. (2007). Primary source attribution and analysis of α-pinene
831 photooxidation products in Duke Forest, North Carolina. *Atmospheric Environment*, *41*,
832 2958–2966. https://doi.org/10.1016/j.atmosenv.2006.12.018

833 Bonsang, B., Polle, C., & Lambert, G. (1992). Evidence for marine production of isoprene,
834 *Geophysical Research Letter, 19*, 1129−1132. https://doi.org/10.1029/92GL00083

835 Boreddy, S. K. R., & Kawamura, K. (2015). A 12-year observation of water-soluble ions in
836 TSP aerosols collected at a remote marine location in the western North Pacific: an
837 outflow region of Asian dust. *Atmospheric Chemistry and Physics*, *15*, 6437–6453.
838 https://doi:org/10.5194/acp-15-6437-2015

839 Boreddy, S. K. R., Haque, M., & Kawamura, K. (2018). Long-term (2001-2012) trends of
840 carbonaceous aerosols from remote island in the western North Pacific: an outflow region
841 of Asian pollutants and dust. *Atmospheric Chemistry and Physics*, *18*, 1291–1306.
842 https://doi:org/10.5194/acp-18-1291-2018

843 Bourgeois, Q., & Bey, I. (2011) Pollution transport efficiency toward the Arctic: Sensitivity to
844 aerosol scavenging and source regions. *Journal of Geophysical Research: Atmospheres*,
845 *116*, D08213. https//:doi: 10.1029/2010JD015096

846 Broadgate, W. J., Liss, P. S., & Penkett, S. A. (1997). Seasonal emissions of isoprene and other
847 reactive hydrocarbon gases from the ocean. *Geophysical Research Letter*, *24*, 2675−2678.
848 https://doi.org/10.1029/97GL02736

849 Brown, S. S., deGouw, J. A., Warneke, C., Ryerson, T. B., Dube´, W. P., Atlas, E., Weber, R.
850 J., Peltier, R. E., Neuman, J. A., Roberts, J. M., Swanson, A., Flocke, F., McKeen, S. A.,
851 Brioude, J., Sommariva, R., Trainer, M., Fehsenfeld, F. C., & Ravishankara, A. R. (2009).
852 Nocturnal isoprene oxidation over the Northeast United States in summer and its impact
853 on reactive nitrogen partitioning and secondary organic aerosol. *Atmospheric Chemistry*
854 *and Physics*, *9,* 3027– 3042. https://doi:10.5194/acp-9-3027-2009

855 Chen, J., Kawamura, K., Liu, C. Q., & Fu, P. Q. (2013). Long-term observations of saccharides
856 in remote marine aerosols from the western North Pacific: A comparison between 1990-
857 1993 and 2006-2009 periods. *Atmospheric Environment*, *67*, 448-458.
858 https://doi:10.1016/j.atmosenv.2012.11.014

859 Ciccioli, P., Centritto, M., & Loreto, F. (2014). Biogenic volatile organic compound emissions
860 from vegetation fires. *Plant, Cell and Environment, 37*, 1810–1825.
861 https://doi.10.1111/pce.12336

862 Claeys, M., Graham, B., Vas, G., Wang, W., Vermeylen, R., Pashynska, V., Cafmeyer, J.,
863 Guyon, P., Andreae, M. O., Artaxo, P., & Maenhaut, W. (2004). Formation of secondary
864 organic aerosols through photooxidation of isoprene. *Science*, *303*, 1173–1176.
865 https://doi:10.1126/ science.1092805

866 Claeys, M., Szmigielski, R., Kourtchev, I., van der Veken, P., Vermeylen, R., Maenhaut, W.,
867 Jaoui, M., Kleindienst, T. E., Lewandowski, M., Offenberg, J. H., & Edney, E. O. (2007).
868 Hydroxydicarboxylic acids: markers for secondary organic aerosol from the
869 photooxidation of a-pinene. *Environmental Science and Technology*, *41,* 1628-1634.
870 https://doi: 10.1021/es0620181

871 de Gouw, J., & Jimenez, J. L. (2009). Organic aerosols in the Earth's atmosphere.

Environmental Science and Technology, *43*, 7614-7618. https://doi:10.1021/es9006004

de Lillis M., Bianco P.M., & Loreto F. (2009). The influence of leaf water content and isoprenoids on flammability of some Mediterranean woody species. *International Journal of Wildland Fire, 18*, 203–212. https://doi.10.1071/WF07075

Ding, X., He, Q.-F., Shen, R.-Q., Yu, Q.-Q., & Wang, X.-M. (2014). Spatial distributions of secondary organic aerosols from isoprene, monoterpenes, β-caryophyllene, and aromatics over China during summer. *Journal of Geophysical Research: Atmosphere*, *119*, 11877-11891. https://doi.org/10.1002/2014JD021748

Ding, X., Wang, X. M., Xie, Z. Q., Zhang, Z., & Sun, L. G. (2013). Impacts of Siberian biomass burning on organic aerosols over the North Pacific Ocean and the Arctic: Primary and secondary organic tracers. *Environmental Science and Technology*, *47*(7), 3149-3157. https://doi:10.1021/es3037093

Ding, X., Wang, X., Gao, B. Fu, X., He, Q., Zhao, X., Yu, J., & Zheng M. (2012). Tracer based estimation of secondary organic carbon in the Pearl River Delta, South China. *Journal of Geophysical Research, 117*, DO5313. https://doi.org/10.1029/2011JD016596

Ding, X., Wang, X.M., & Zheng, M. (2011). The influence of temperature and aerosol acidity on biogenic secondary organic aerosol tracers: observations at a rural site in the central Pearl River Delta region, South China. *Atmospheric Environment*, *45*, 1303-1311. https://doi.org/10.1016/j.atmosenv.2010.11.057

Draxler, R. R., & Rolph, G. D. (2013). HYSPLIT (HYbrid Single–Particle Lagrangian Integrated Trajectory) Model, access via NOAA ARL READY Website, available at: https://ready.arl.noaa.gov/ HYSPLIT traj.php.

Fall R. (1999). Biogenic emissions of volatile organic compounds from higher plants. *In Reactive Hydrocarbons in the Atmosphere* (ed C.N. Hewitt), pp. 41–86. Academic Press, San Diego, CA. https://doi.org/10.1016/B978-012346240-4/50003-5

Fowler, D., Pilegaard, K., Sutton, M. A., Ambus, P., Raivonen, M., & Duyzer, J. (2009). Atmospheric composition change: Ecosystems-Atmosphere interactions. *Atmospheric Environment*, *43* (33), 5193−5267. https://doi:10.1016/j.atmosenv.2009.07.068

Fu, P. Q., Kawamura, K., & Miura, K. (2011). Molecular characterization of marine organic aerosols collected during a round-the-world cruise. *Journal of Geophysical Research: Atmosphere*, *116*, D13302. https://doi:org/10.1029/2011JD015604

Fu, P. Q., Kawamura, K., Okuzawa, K., Aggarwal, S. G., Wang, G. H., Kanaya, Y., Wang, Z. (2008). Organic molecular compositions and temporal variations of summertime mountain aerosols over Mt. Tai, North China Plain. *Journal of Geophysical Research: Atmosphere*, *113* D19107. https://doi:10.1029/2008jd009900

Fu, P., Aggarwal, S. G., Chen, J., Li, J., Sun, Y., Wang, Z., Chen, H., Liao, H., Ding, A., Umarji, G. S., Patil, R. S., Chen, Q., & Kawamura, K. (2016). Molecular markers of secondary organic aerosol in Mumbai, India. *Environmental Science & Technology*, *50*, 4659– 4667. https://doi.org/10.1021/acs.est.6b00372

Glasius, M., Lahaniati, M., Calogirou, A., Di Bella, D., Jensen, N. R., Hjorth, J., Kotzias, D., & Larsen, B. R. (2000). Carboxylic acids in secondary aerosols from oxidation of cyclic monoterpenes by ozone. *Environmental Science & Technology*, *34*, 1001–1010. https://doi.org/10.1021/es990445r

Goldstein, A. H., & Galbally, I. E. (2007). Known and unexplored organic constituents in the earth's atmosphere. *Environmental Science and Technology*, *41*, 1514-1521. https://doi:10.1021/es072476p

Griffin, R. J., Cocker, D. R., Seinfeld, J. H., & Dabdub, D. (1999). Estimate of global

atmospheric organic aerosol from oxidation of biogenic hydrocarbons. *Geophysical Research Letters*, *26*, 2721–2724. https://doi.org/10.1029/1999GL900476

Guenther, A., Hewitt, N. C., Erickson, D., Fall, R., Geron, C., Graedel, T., Harley, P., Klinger, L., Lerdau, M., Mckay, W. A., Pierce, T., Scholes, B., Steinbrecher, R., Tallamraju, R., Taylor, J., & Zimmerman, P. (1995). A global model of natural volatile organic compound emissions. *Journal of Geophyscal Ressearch: Atmospheres, 100*, 8873–8892. https://doi:10.1029/94JD02950

Guenther, A., Karl, T., Harley, P., Wiedinmyer, C., Palmer, P., & Geron, C. (2006). Estimates of global terrestrial isoprene emissions using MEGAN (Model of Emissions of Gases and Aerosols from Nature). *Atmospheric Chemistry and Physics, 6*, 3181-3210. https://dx.doi.org/10.5194/acp-6-3181-2006

Hackenberg, S. C., Andrews, S. J., Airs, R., Arnold, S. R., Bouman, H. A., Brewin, R. J. W., Chance, R. J., Cummings, D., Dall'Olmo, G., Lewis, A. C., Minaeian, J. K., Reifel, K. M., Small, A., Tarran, G. A., Tilstone, G. H., & Carpenter, L. J. (2017). Potential controls of isoprene in the surface ocean. *Global Biogeochemical Cycle*, *31*, 644–662. https://doi.org/10.1002/2016GB005531-2017

Hallquist, M., Wenger, J. C., Baltensperger, U., Rudich, Y., Simpson, D., & Claeys M. (2009). The formation, properties and impact of secondary organic aerosol: current and emerging issues. *Atmospheric Chemistry and Physics*, *9*, 5155–5236. https://doi:10.5194/acp-9-5155-2009

Han, F., Kota, S. H., Wang, Y., & Zhang, H. (2017). Source apportionment of $PM_{2.5}$ in Baton Rouge, Louisiana during 2009–2014. *Science of the Total Environment, 586,* 115–126. https://doi.org/10.1016/j.scitotenv.2017.01.189

Heald, C. L., Jacob, D. J., Park, R. J., Russell, L. M., Huebert, B. J. Seinfeld, J. H., Liao, H., & Weber, R. J. (2005). A large organic aerosol source in the free troposphere missing from current models. *Geophysical Research Letters, 32,* L18809. https://doi:10.1029/2005GL023831

Henze, D. K., & Seinfeld, J. H. (2006). Global secondary organic aerosol from isoprene oxidation. *Geophysical Research Letters, 45*, 6972–6982. https://doi.org/10.1029/2018GL078689

Hoffmann, T., Odum, J. R., Bowman, F., Collins, D., Klockow, D., Flagan, R. C., & Seinfeld, J. H. (1997). Formation of organic aerosols from the oxidation of biogenic hydrocarbons. *Journal of Atmospheric Chemistry*, *26*, 189–222. https://doi.org/10.1023/A:1005734301837

Hoyle, C. R., Berntsen, T., Myhre, G., & Isaksen, I. S. A. (2007). Secondary organic aerosol in the global aerosol-chemical transport model Oslo CTM2. *Atmospheric Chemistry and Physics*, 7, 5675–5694. http://doi:10.5194/acp-7-5675-2007

Hoyle, C. R., Boy, M., Donahue, N. M., Fry, J. L., Glasius, M., Guenther, A., Hallar, A. G., Huff Hartz, K., Petters, M. D., Peta ja, T., Rosenoern, T., & Sullivan, A. P. (2011). A review of the anthropogenic influence on biogenic secondary organic aerosol. *Atmospheric Chemistry and Physics*, *11*, 321–343, 2011. https://doi:10.5194/acp-11-321-2011

Iinuma, Y., Böge, O., Gnauk, T., & Herrmann, H. (2004). Aerosol-chamber study of the α-pinene/O_3 reaction: influence of particle acidity on aerosol yields and products. *Atmospheric Environment*, *38*, 761–773. https://doi.org/10.1016/j.atmosenv.2003.10.015

Intergovernmental Panel on Climate Change (IPCC): Climate Change: The Scientific Basis, Cambridge University Press, UK, 2001.

Jaoui, M., Lewandowski, M., Kleindienst, T. E., Offenberg, J. H., & Edney, E. O. (2007). β-Caryophyllinic acid: An atmospheric tracer for β-caryophyllene secondary organic aerosol.

967 *Geophysical Research Letters. 34*, L05816. https://doi:10.1029/2006GL028827
968 Kanakidou, M., Seinfeld, J. H., Pandis, S. N., Barnes, I., Dentener, F. J., & Facchini, M. C.
969 (2005). Organic aerosol and global climate modelling: A review. *Atmospheric Chemistry*
970 *and Physics*, *5*, 1053–1123. https://doi:10.5194/acp-5-1053-2005
971 Kang, M., Fu, P.Q., Kawamura, K., Yang, F., Zhang, H., Zang, Z., Ren, H., Ren, L., Zhao, Y.
972 Sun, Y., & Wang, Z. (2018). Characterization of biogenic primary and secondary organic
973 aerosols in the marine atmosphere over the East China Sea. *Atmospheric Chemistry and*
974 *Physics*, *18*, 13947–13967. https://doi.org/10.5194/acp-18-13947-2018
975 Kavouras, I. G., Mihalopoulos, N., & Stephanou, E. G. (1998). Formation of atmospheric
976 particles from organic acids produced by forests. *Nature*, *395*, 683–686.
977 https://doi:10.1038/27179
978 Kawamura, K., Ishimura, Y., & Yamazaki, K. (2003). Four years' observations of terrestrial
979 lipid class compounds in marine aerosols from the western North Pacific. *Global*
980 *Biogeochemical Cycles*, *17*(1), 1003. https://doi:10.1029/2001gb001810
981 Keeling C.I., & Bohlmann J. (2006). Genes, enzymes and chemicals of terpenoid diversity in
982 the constitutive and induced defense of conifers against insects and pathogens. *New*
983 *Phytologist*, *170***,** 657–675. https://doi.10.1111/j.1469-8137.2006.01716.x
984 Kim, J. C. (2001). Factors controlling natural VOC emissions in a southeastern US pine forest.
985 *Atmospheric Environment*, *35*, 3279-3292. https://doi:10.1016/S1352-2310(00)00522-7
986 Kleindienst, T. E., Jaoui, M., Lewandowski, M., Offenberg, J. H., Lewis, C. W., & Bhave, P. V.
987 (2007). Estimates of the contributions of biogenic and anthropogenic hydrocarbons to
988 secondary organic aerosol at a southeastern US location. *Atmospheric Environment*, *41*,
989 8288-8300. https://doi.org/10.1016/j.atmosenv.2007.06.045
990 Kleindienst, T. E., Lewandowski, M., Offenberg, J. H., Jaoui, M., & Edney, E. O. (2009). The
991 formation of secondary organic aerosol from the isoprene plus OH reaction in the absence
992 of NO_x. *Atmospheric Chemistry Physics*, *9*, 6541-6558. https://doi.org/10.5194/acp-9-
993 6541-2009
994 Kourtchev, I., Warnke, J., Maenhaut, W., Hoffmann, T., & Claeys, M. (2008). Polar organic
995 marker compounds in $PM_{2.5}$ aerosol from a mixed forest site in western Germany.
996 *Chemosphere*, *73*, 1308-1314. https://doi.org/10.1016/j.chemosphere.2008.07.011
997 Kulmala, M., Asmi, A., Lappalainen, H. K., Baltensperger, U., Brenguier, J.-L., Facchini, M.
998 C., Hansson, H.-C., Hov, Ø., O'Dowd, C. D., Pöschl, U., Wiedensohler, A., Boers, R.,
999 Boucher, O., de Leeuw, G., Denier van der Gon, H. A. C., Feichter, J., Krejci, R., Laj, P.,
1000 Lihavainen, H., Lohmann, U., McFiggans, G., Mentel, T., Pilinis, C., Riipinen, I., Schulz,
1001 M., Stohl, A., Swietlicki, E., Vignati, E., Alves, C., Amann, M., Ammann, M., Arabas, S.,
1002 Artaxo, P., Baars, H., Beddows, D. C. S., Bergström, R., Beukes, J. P., Bilde, M., Burkhart,
1003 J. F., Canonaco, F., Clegg, S. L., Coe, H., Crumeyrolle, S., D'Anna, B., Decesari, S.,
1004 Gilardoni, S., Fischer, M., Fjaeraa, A. M., Fountoukis, C., George, C., Gomes, L.,
1005 Halloran, P., Hamburger, T., Harrison, R. M., Herrmann, H., Hoffmann, T., Hoose, C., Hu,
1006 M., Hyvärinen, A., Hõrrak, U., Iinuma, Y., Iversen, T., Josipovic, M., Kanakidou, M.,
1007 Kiendler-Scharr, A., Kirkevåg, A., Kiss, G., Klimont, Z., Kolmonen, P., Komppula, M.,
1008 Kristjánsson, J.-E., Laakso, L., Laaksonen, A., Labonnote, L., Lanz, V. A., Lehtinen, K. E.
1009 J., Rizzo, L. V., Makkonen, R., Manninen, H. E., McMeeking, G., Merikanto, J., Minikin,
1010 A., Mirme, S., Morgan, W. T., Nemitz, E., O'Donnell, D., Panwar, T. S., Pawlowska, H.,
1011 Petzold, A., Pienaar, J. J., Pio, C., Plass-Duelmer, C., Prévôt, A. S. H., Pryor, S.,
1012 Reddington, C. L., Roberts, G., Rosenfeld, D., Schwarz, J., Seland, Ø., Sellegri, K., Shen,
1013 X. J., Shiraiwa, M., Siebert, H., Sierau, B., Simpson, D., Sun, J. Y., Topping, D., Tunved,
1014 P., Vaattovaara, P., Vakkari, V., Veefkind, J. P., Visschedijk, A., Vuollekoski, H., Vuolo,

R., Wehner, B., Wildt, J., Woodward, S., Worsnop, D. R., van Zadelhoff, G.-J., Zardini, A. A., Zhang, K., van Zyl, P. G., Kerminen, V.-M., S Carslaw, K., & Pandis, S. N. (2011). General overview: European integrated project on aerosol cloud climate and air quality interactions (EUCAARI)–integrating aerosol research from nano to global scales. *Atmospheric Chemistry Physics*, *11*, 13061–13143. https://doi.org/10.5194/acp-11-13061-2011

Kurihara, M. K., Kimura, M., Iwamoto, Y., Narita, Y., Ooki, A., Eum, Y.-J., Tsuda, A., Suzuki, K., Tani, Y., Yokouchi, Y., Uematsu, M., & Hashimoto, S. (2010). Distributions of short-lived iodocarbons and biogenic trace gases in the open ocean and atmosphere in the western North Pacific. *Marine Chemistry*, *118*(3–4), 156–170. https://doi:10.1016/j.marchem.2009.12.001

Lewandowski, M., Piletic, I. R., Kleindienst, T. E., Offenberg, J. H. ,Beaver, M. R., Jaoui, M. et. al. (2013). Secondary organic aerosol characterisation at field sites across the United States during the spring–summer period. *International Journal of Environmental Analytical Chemistry, 93*, 1084–1103. https://doi.org/10.1080/03067319.2013.803545

Li, Z., Ratliff, E. A., & Sharkey, T. D. (2011). Effect of temperature on postillumination isoprene emission in oak and poplar. *Plant Physiology*, *155* (2), 1037-1046. https://doi/10.1104/pp.110.167551

Lopez-Hilfiker, F. D., Mohr, C., D'Ambro, E. L., Lutz, A., Riedel, T. P., Gaston, C. J., Iyer, S., Zhang, Z., Gold, A., Surratt, J. D., & Lee, B. H. (2016). Molecular composition and volatility of organic aerosol in the southeastern US: Implications for IEPOX derived SOA. *Environmental Science & Technology*, *50*, 2200–2209. https://doi.org/10.1021/acs.est.5b04769

Mentel, Th. F., Kleist, E., Andres, S., Maso, M. D., Hohaus, T., Kiendler-Scharr, A., Rudich, Y., Springer, M., Tillmann, R., Uerlings, R., Wahner, A., & Wildt, J. (2013). Secondary aerosol formation from stress-induced biogenic emissions and possible climate feedbacks. *Atmospheric Chemistry and Physics, 13,* 8755–8770. https://doi:10.5194/acp-13-8755-2013

Meskhidze, N., & Nenes, A. (2006). Phytoplankton and cloudiness in the Southern Ocean. *Science*, *314*, 1419–1423. http://doi:10.1126/science.1131779

Mochida, M., Kawamura, K., Fu, P. Q., & Takemura, T. (2010). Seasonal variation of levoglucosan in aerosols over the western North Pacific and its assessment as a biomass-burning tracer. *Atmospheric Environment*, *44*(29), 3511-3518. https://doi.org/10.1016/j.atmosenv.2010.06.017

Ng, N. L., Kwan, A. J., Surratt, J. D., Chan, A. W. H., Chhabra, P. S., Sorooshian, A., Pye, H. O. T., Crounse, J. D., Wennberg, P. O., Flagan, R. C., & Seinfeld, J. H. (2008). Secondary organic aerosol (SOA) formation from reaction of isoprene with nitrate radicals (NO_3). *Atmospheric Chemistry and Physics, 8,* 4117–4140. https//:doi:10.5194/acpd-8-3163-2008

Ooki, A., Nomura, D., Nishino, S., Kikuchi, T., & Yokouchi, Y. (2015). A global-scale map of isoprene and volatile organic iodine in surface seawater of the Arctic, Northwest Pacific, Indian, and Southern Oceans. *Journal Geophysical Research Oceans*, *120*, 4108–4128. https://doi:10.1002/2014JC010519

Paatero, P., & Tapper, U. (1994). Positive matrix factorization: a non-negative factor model with optimal utilization of error estimates of data values. *Environmetrics, 5,* 111-126. https://dx.doi.org/10.1002/env.3170050203

Paatero, P., Hopke, P. K., Song, X. H., & Ramadan, Z. (2002). Understanding and controlling rotations in factor analytic models. *Chemometrics and Intelligent Laboratory Systems, 60*, 253–264, 2002. https://doi.org/10.1016/S0169-7439(01)00200-3

1063 Piccot, S., Watson, J., & Jones, J. (1992). A global inventory of volatile organic compound
1064 emissions from anthropogenic sources. *Journal of Geophysical Research: Atmospheric*,
1065 *97(D9)*, 9897–9912. https://doi:10.1029/92JD00682

1066 Rasulov, B., Hüve, K., Bichele, I., Laisk, A., & Niinemets, Ü. (2010). Temperature response of
1067 isoprene emission in vivo reflects a combined effect of substrate limitations and isoprene
1068 synthase activity: a kinetic analysis. *Plant Physiolology*, *154* (3), 1558–1570.
1069 https://doi:10.1104/pp.110.162081

1070 Riva, M., Budisulistiorini, S. H., Zhang, Z., Gold, A., & Surratt, J. D. (2016). Chemical
1071 characterization of secondary organic aerosol constituents from isoprene ozonolysis in the
1072 presence of acidic aerosol. *Atmospheric Environment*, *130*, 5–13.
1073 https//:doi:10.1016/j.atmosenv.2015.06.027

1074 Robinson, A.L., Donahue, N. M., & Rogge, W. F. (2006). Photochemical oxidation and
1075 changes in molecular composition of organic aerosol in the regional context. *Journal of*
1076 *Geophysical Research: Atmosphere*, *111*, D03302. https://doi.org/10.1029/2005JD006265

1077 Sekimoto K., Koss, A. R., Gilman, J. B., Selimovic, V., Coggon, M. M., Zarzana, K. J., Yuan,
1078 B., Lerner, B. M., Brown, S. S., Warneke, C., Yokelson, R. J., Roberts, J. M., & de Gouw,
1079 J. (2018). High- and low-temperature pyrolysis profiles describe volatile organic
1080 compound emissions from western US wildfire fuels. *Atmospheric Chemistry and Physics*,
1081 *18*, 9263-9281. https://doi.org/10.5194/acp-18-9263-2018

1082 Sharkey, T. D., & Singsaas, E. L. (1995). Why plants emit isoprene. *Nature*, *374* (6525), 769–
1083 769. https://doi:10.1038/374769a0

1084 Shaw, S. L., Chisholm, S. W., & Prinn, R. G. (2003). Isoprene production by Prochlorococcus,
1085 a marine cyanobacterium, and other phyto-plankton. *Marine Chemistry*, *80*, 227–245.
1086 https://doi.org/10.1016/S0304-4203(02)00101-9

1087 Simoneit, B. R. T., Kobayashi, M., Mochida, M., Kawamura, K., Lee, M., Lim, H. J., Turpin,
1088 B. J., & Komazaki, Y. (2004). Composition and major sources of organic compounds of
1089 aerosol particulate matter sampled during the ACE-Asia campaign. *Journal of*
1090 *Geophysical Research: Atmospheres*, *109*(D19). https://doi:10.1029/2004jd004598

1091 Stone, E. A., Hedman, C. J., Zhou, J., Mieritz, M., & Schauer, J. J. (2010). Insights into the
1092 nature of secondary organic aerosol in Mexico City during the MILAGRO experiment.
1093 *Atmospheric Environment, 44*, 312-319. https://doi:org/10.1016/j.atmosenv.2009.10.036

1094 Stone, E. A., Nguyen, T. T., Pradhan, B. B., & Dangol, P. M. (2012). Assessment of biogenic
1095 secondary organic aerosol in the Himalayas. *Environmental Chemistry*, *9,* 263–272, 2012.
1096 https//:doi:10.1071/EN12002

1097 Surratt, J. D., Chan, A. W. H., Eddingsaas, N. C., Chan, M. N., Loza, C. L., & , A. J. (2010).
1098 Reactive intermediates revealed in secondary organic aerosol formation from isoprene.
1099 *Proceedings of the National Academy Science United Status of America, 107*(15), 6640-
1100 6645. https://doi:org/10.1073/pnas.0911114107

1101 Surratt, J. D., Murphy, S. M., Kroll, J. H., Ng, N. L., Hildebrandt, L., Sorooshian, A.,
1102 Szmigielski, R., Vermeylen, R., Maenhaut, W., Claeys, M., Flagan, R. C., Seinfeld, J. H.
1103 (2006). Chemical composition of secondary organic aerosol formed from the
1104 photooxidation of isoprene. *Journal of Physical Chemistry A*, *110*, 9665-9690.
1105 https://doi:10.1021/jp061734m

1106 Szmigielski, R., Surratt, J. D., Gómez-González, Y., van der Veken, P., Kourtchev, I.,
1107 Vermeylen, R., Blockhuys, F., Jaoui, M., Kleindienst, T. E., Lewandowski, M., Offenberg,
1108 J. H., Edney, E. O., Seinfeld, J. H., Maenhaut, W., & Claeys, M. (2007). 3-methyl-1,2,3-
1109 butanetricarboxylic acid: An atmospheric tracer for terpene secondary organic aerosol.
1110 *Geophysical Research Letters*, *34(24)*, L24811. https://doi:10.1029/2007GL031338

Verma, S. K., Kawamura, K., Chen, J., & Fu, P. Q. (2018). Thirteen years of observations on primary sugars and sugar alcohols over remote Chichijima Island in the western North Pacific. *Atmospheric Chemistry Physics, 18*, 81–101. https://doi:org/10.5194/acp-18-81-2018

Verma, S. K., Kawamura, K., Chen, J., Fu, P. Q., & Zhu, C. M. (2015). Thirteen years of observations on biomass burning organic tracers over Chichijima Island in the western North Pacific: an outflow region of Asian aerosols. *Journal of Geophysical Research: Atmospheres, 120*, 4155-4168. https://doi.org/10.1002/2014JD022224

von Schneidemesser, E., Zhou, J., Stone, E. A., Schauer, J. J., Shpund, J., Brenner, S., Qasrawi, R., Abdeen, Z., & Sarnat, J. A. (2009). Spatial variability of carbonaceous aerosol concentrations in east and west Jerusalem. *Environmental Science and Technology, 44*, 1911–1917. https://doi:10.1021/es9014025

Wang, G. H., Kawamura, K., & Lee, M. (2009). Comparison of organic compositions in dust storm and normal aerosol samples collected at Gosan, Jeju Island, during spring 2005. *Atmospheric Environment*, *43*(2), 219-227. https://doi:10.1016/j.atmosenv.2008.09.046

Wang, W., Wu, M. H., Li, L., Zhang, T., Liu, X.D., Feng, J. L., Li, H.J., Wang, Y. J., Sheng, G. Y., Claeys, M., & Fu, J. M. (2008). Polar organic tracers in $PM_{2.5}$ aerosols from forests in eastern China. *Atmospheric Chemistry and Physics*, *8*, 7507-7518. https://doi.org/10.5194/acp-8-7507-2008

Xia, X., & Hopke, P. K. (2006). Seasonal Variation of 2-Methyltetrols in Ambient Air Samples. *Environmental Science and Technology 40* (22), 6934-7. https://doi.10.1021/es060988i

Xie, M., Hannigan, M. P., & Barsanti, K. C. (2014). Gas/Particle partitioning of 2-methyltetrols and levoglucosan at an urban site in Denver. *Environmental Science and Technology, 48*, 2835–2842. https://doi.org/10.1021/es405356n

Yamamoto, S., Kawamura, K., & Seki, O. (2011). Long-range atmospheric transport of terrestrial biomarkers by the Asian winter monsoon: Evidence from fresh snow from Sapporo, northern Japan. *Atmospheric Environment, 45*, 3553–3560. https://doi.org/10.1016/j.atmosenv.2011.03.071

Zhang, J. Y., & Wu, L. Y. (2011). Land-atmosphere coupling amplifies hot extremes over China. *Chinese Science Bulletin*, *56*(31), 3328-3332. https://doi:10.1007/s11434-011-4628-3

Zhou, L., Kim, E., Hopke, P. K., Stanier, C. O., & Pandis, S. (2004). Advanced factor analysis on Pittsburgh particle size-distribution data special issue of aerosol science and technology on findings from the fine particulate matter supersites program. *Aerosol Science and Technology, 38*, 118–132. https://doi.org/10.1080/02786820390229589

Zhu, C., Kawamura, K., & Fu, P. (2016). Seasonal variations of biogenic secondary organic aerosol tracers in Cape Hedo, Okinawa. *Atmospheric Environment*, *130*, 113–119. https://doi:org/10.1016/j.atmosenv.2015.08.069

Figure Captions

Figure 1. Geographic location of Chichijima Island (27.06°N and 142.21°E) in the western North Pacific. Sampling site is indicated by the red star.

Figure 2. Monthly variation of the meteorological parameters over Chichijima Island during 2010–2012 period (The error bars denote the standard deviations).

Figure 3. Seasonal air-mass backward tracjectories over Chichijima Island during winter (December–February), spring (March–May), summer (June–August), and autumn (September–November).

Figure 4. Temporal trends of measured SOA tracers at Chichijima Island during the campaign.

Figure 5. Monthly trends of measured SOA tracers at Chichijima Island during the campaign.

Figure 6. Seasonal scatter plots of levoglucosan with 2-MTLs (a, b) and *c*SOA tracers (c - g).

Figure 7. Seasonal scatter plots of C_5-alkene triols with 2-MTLs (a - d), 3-MBTCA with 3-HGA (e - h), NO_3^- with 3-HGA (i), and 3-MBTCA (j).

Figure 8. Monthly average concentrations (2010–2012) of levoglucosan and *β*-caryophyllene-SOA tracer in the Chichijima aerosols.

Figure 9. PMF analyses of the biogenic SOA tracers and levoglucosan in the Chichijima aerosols. (levoglucosan data were acquired from Verma et al. (2015) for PMF analysis).

Figure 10. Contributions to biogenic SOA tracers from various sources based on PMF analyses.

Figure 1.

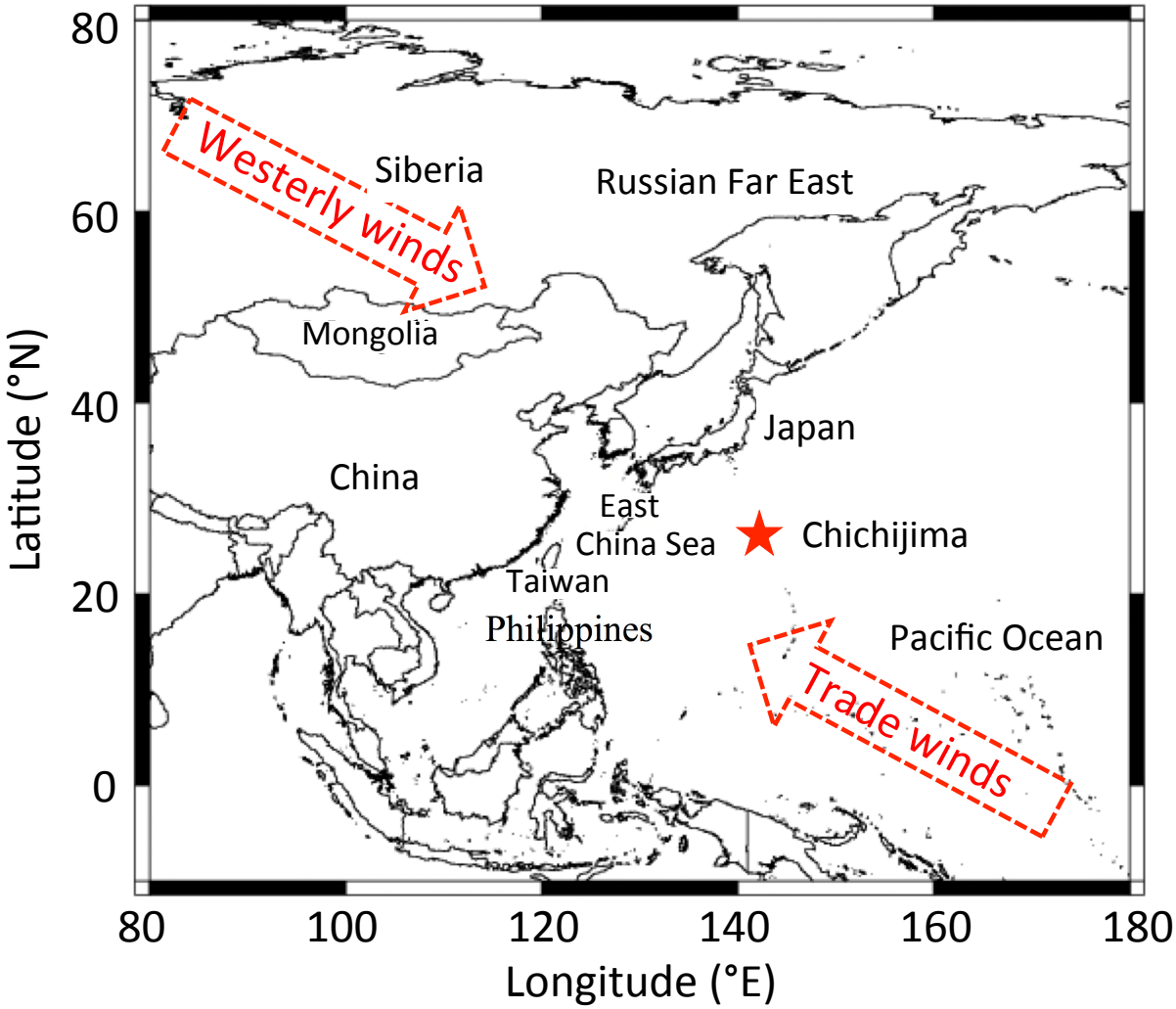
Westerly winds
Siberia
Russian Far East
Mongolia
Japan
China
East
China Sea
Chichijima
Taiwan
Philippines
Pacific Ocean
Trade winds
Latitude (°N)
Longitude (°E)
80
60
40
20
0
80
100
120
140
160
180

Figure 2.

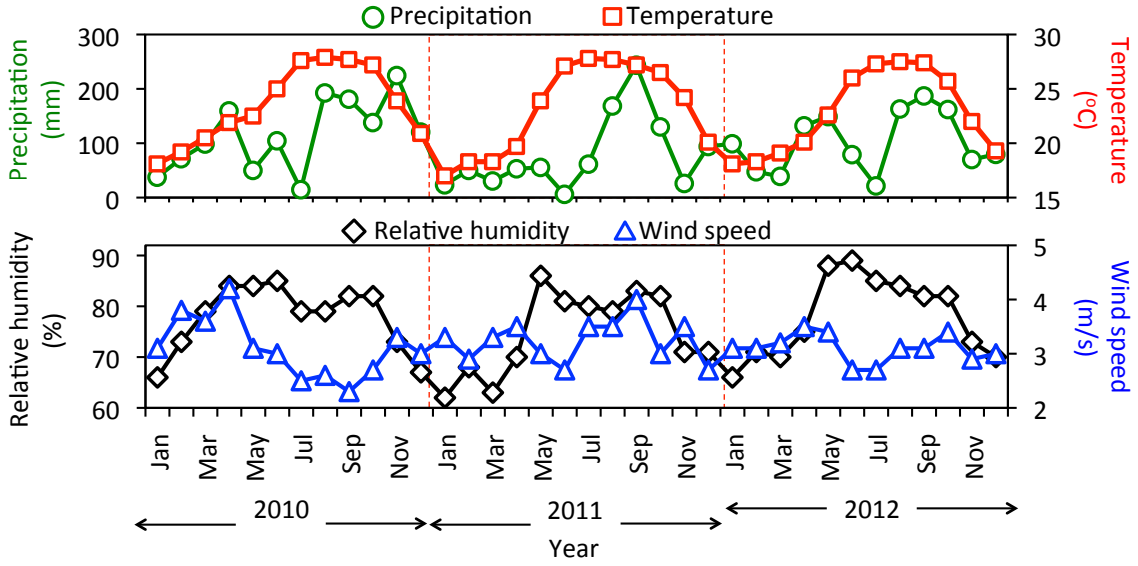
Precipitation
Temperature
Precipitation (mm)
Temperature (°C)
Relative humidity
Wind speed
Relative humidity (%)
Wind speed (m/s)
300
200
100
0
30
25
20
15
90
80
70
60
5
4
3
2
Jan
Mar
May
Jul
Sep
Nov
2010
2011
2012
Year

Figure 3.

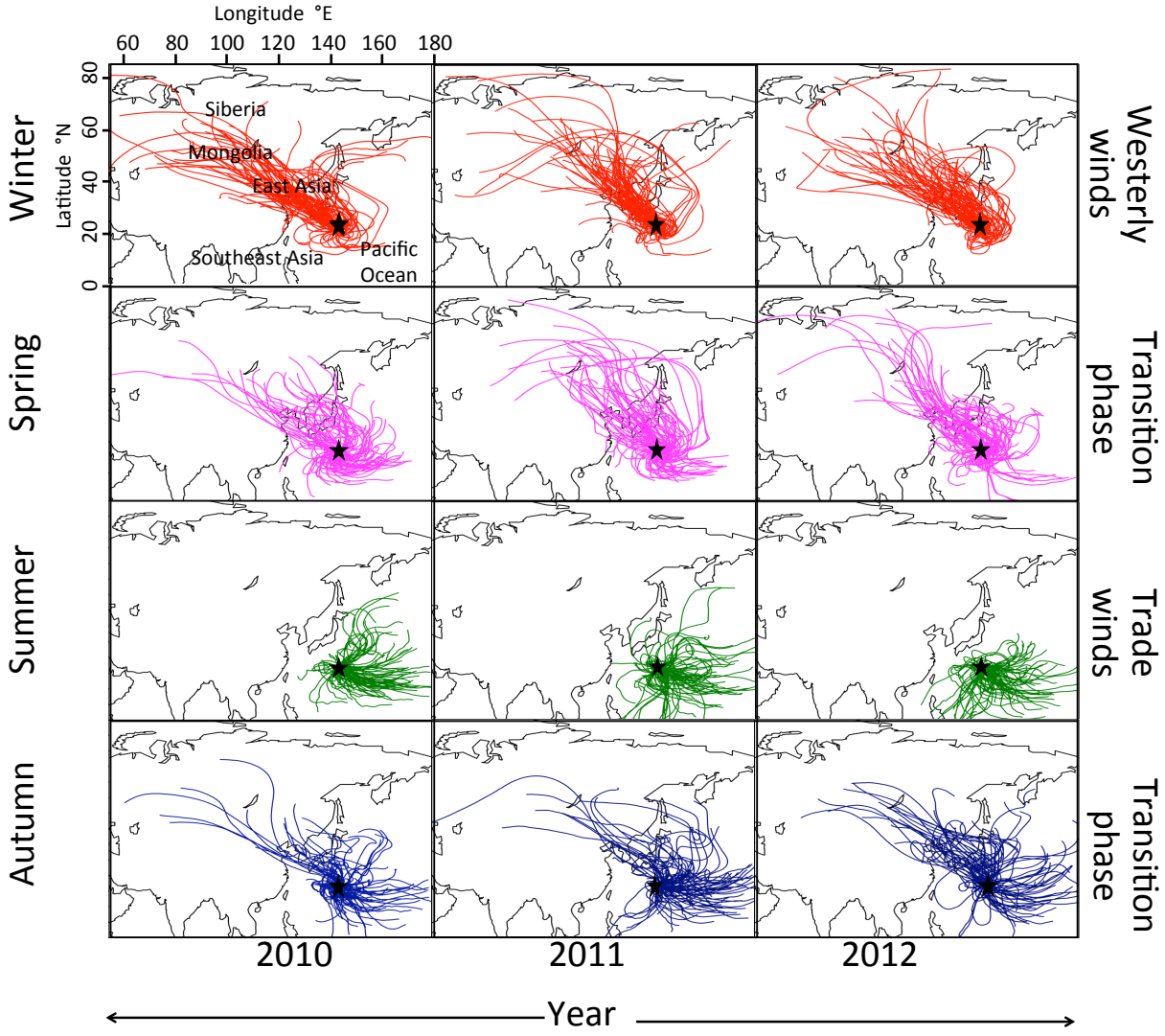
Longitude °E
60
80
100
120
140
160
180
Latitude °N
0
20
40
60
80
Siberia
Mongolia
East Asia
Southeast Asia
Pacific Ocean
Winter
Spring
Summer
Autumn
Westerly winds
Transition phase
Trade winds
Transition phase
2010
2011
2012
Year

Figure 4.

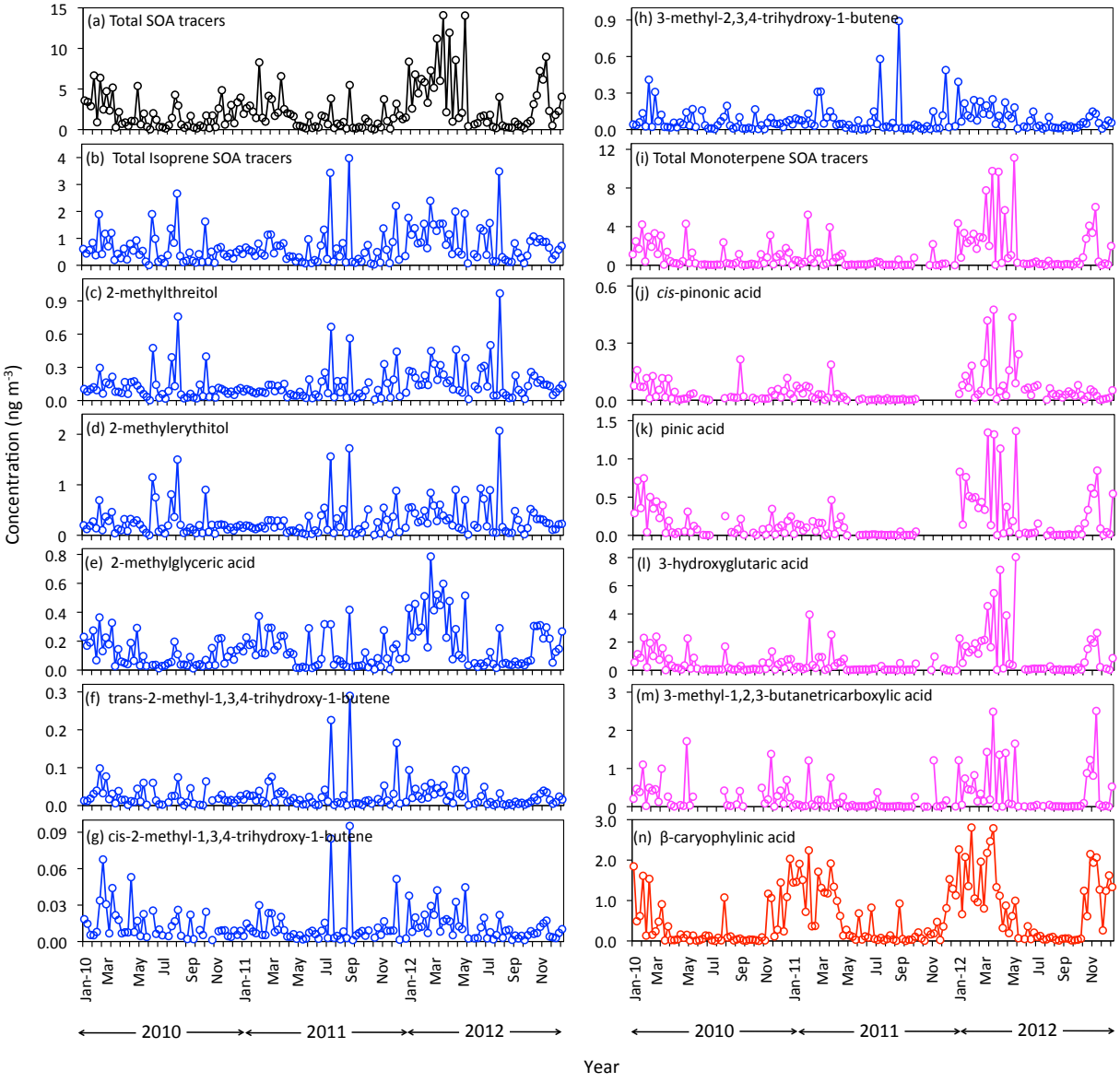
(a) Total SOA tracers
(b) Total Isoprene SOA tracers
(c) 2-methylthreitol
(d) 2-methylerythitol
(e) 2-methylglyceric acid
(f) trans-2-methyl-1,3,4-trihydroxy-1-butene
(g) cis-2-methyl-1,3,4-trihydroxy-1-butene
(h) 3-methyl-2,3,4-trihydroxy-1-butene
(i) Total Monoterpene SOA tracers
(j) cis-pinonic acid
(k) pinic acid
(l) 3-hydroxyglutaric acid
(m) 3-methyl-1,2,3-butanetricarboxylic acid
(n) β-caryophylinic acid
Concentration (ng m-3)
Jan-10 Mar May Jul Sep Nov Jan-11 Mar May Jul Sep Nov Jan-12 Mar May Jul Sep Nov
2010 2011 2012
Year

Figure 5.

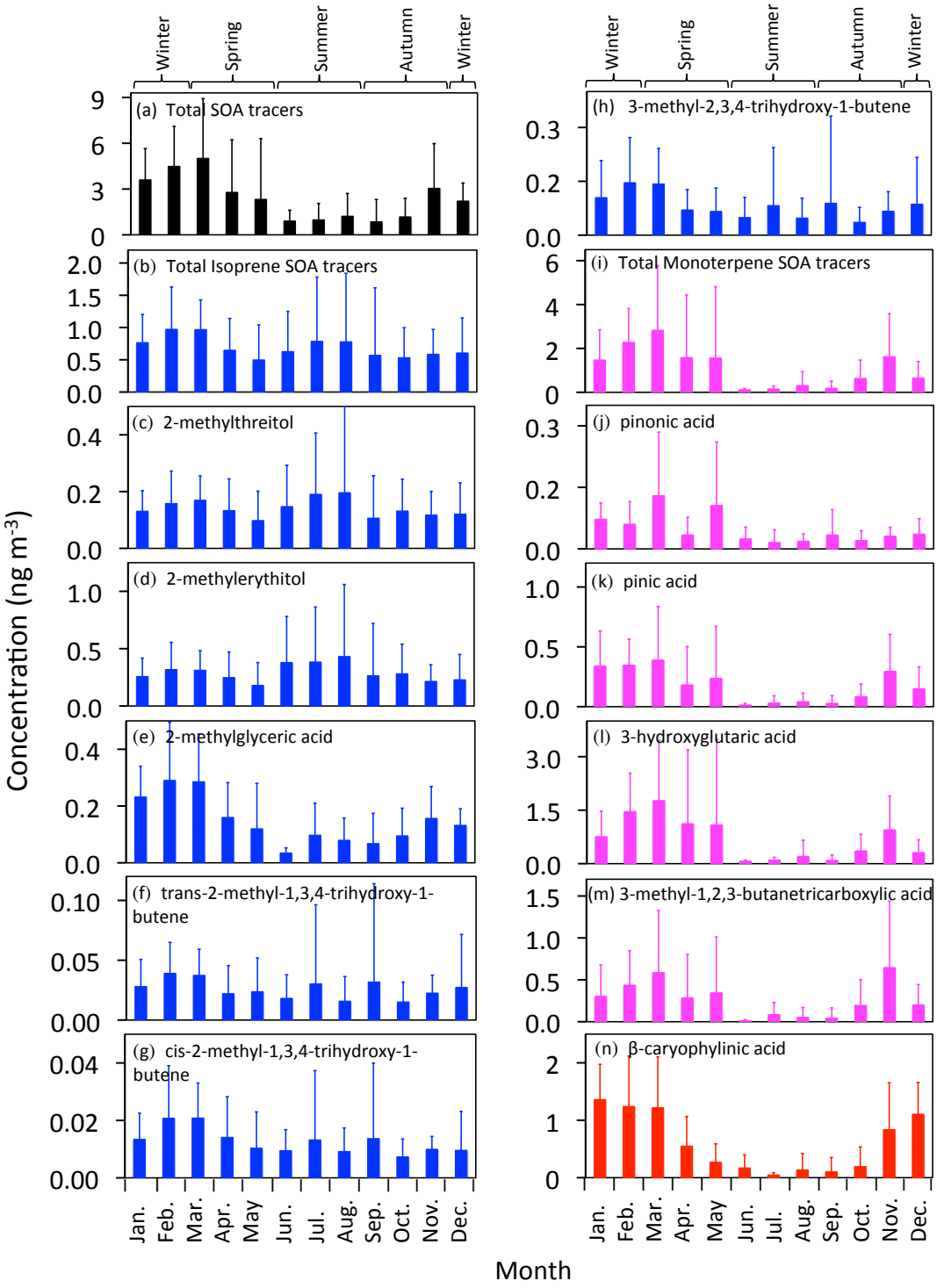
Winter
Spring
Summer
Autumn
Winter
(a) Total SOA tracers
(b) Total Isoprene SOA tracers
(c) 2-methylthreitol
(d) 2-methylerythitol
(e) 2-methylglyceric acid
(f) trans-2-methyl-1,3,4-trihydroxy-1-butene
(g) cis-2-methyl-1,3,4-trihydroxy-1-butene
(h) 3-methyl-2,3,4-trihydroxy-1-butene
(i) Total Monoterpene SOA tracers
(j) pinonic acid
(k) pinic acid
(l) 3-hydroxyglutaric acid
(m) 3-methyl-1,2,3-butanetricarboxylic acid
(n) β-caryophylinic acid
Concentration (ng m-3)
Jan.
Feb.
Mar.
Apr.
May
Jun.
Jul.
Aug.
Sep.
Oct.
Nov.
Dec.
Month

Figure 6.

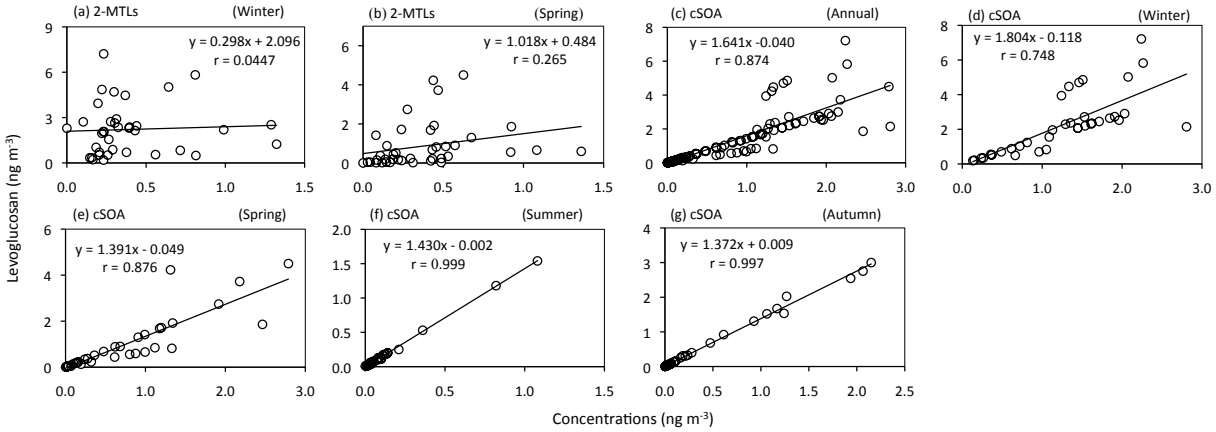
(a) 2-MTLs (Winter)
y = 0.298x + 2.096
r = 0.0447
(b) 2-MTLs (Spring)
y = 1.018x + 0.484
r = 0.265
(c) cSOA (Annual)
y = 1.641x -0.040
r = 0.874
(d) cSOA (Winter)
y = 1.804x - 0.118
r = 0.748
(e) cSOA (Spring)
y = 1.391x - 0.049
r = 0.876
(f) cSOA (Summer)
y = 1.430x - 0.002
r = 0.999
(g) cSOA (Autumn)
y = 1.372x + 0.009
r = 0.997
Levoglucosan (ng m-3)
Concentrations (ng m-3)

Figure 7.

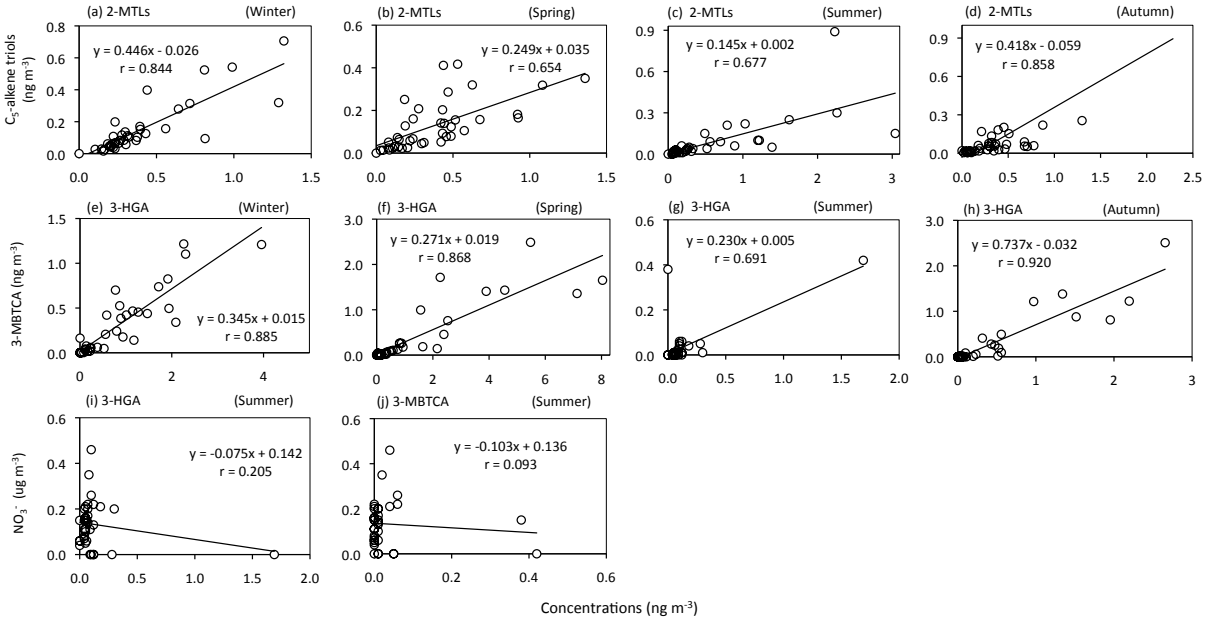
(a) 2-MTLs (Winter)
y = 0.446x - 0.026
r = 0.844
(b) 2-MTLs (Spring)
y = 0.249x + 0.035
r = 0.654
(c) 2-MTLs (Summer)
y = 0.145x + 0.002
r = 0.677
(d) 2-MTLs (Autumn)
y = 0.418x - 0.059
r = 0.858
C5-alkene triols (ng m-3)
(e) 3-HGA (Winter)
y = 0.345x + 0.015
r = 0.885
(f) 3-HGA (Spring)
y = 0.271x + 0.019
r = 0.868
(g) 3-HGA (Summer)
y = 0.230x + 0.005
r = 0.691
(h) 3-HGA (Autumn)
y = 0.737x - 0.032
r = 0.920
3-MBTCA (ng m-3)
(i) 3-HGA (Summer)
y = -0.075x + 0.142
r = 0.205
(j) 3-MBTCA (Summer)
y = -0.103x + 0.136
r = 0.093
NO3- (ug m-3)
Concentrations (ng m-3)

Figure 8.

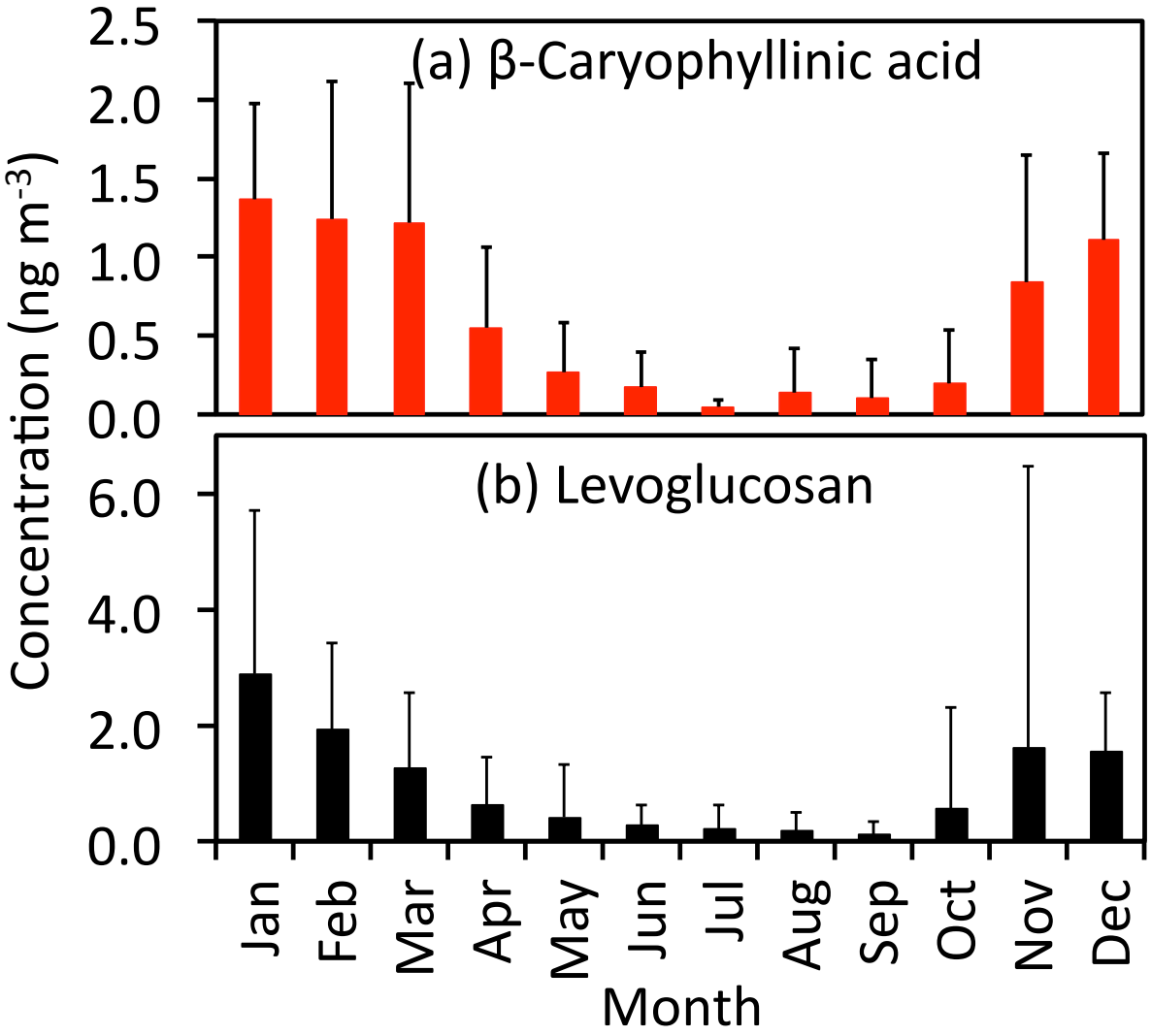
(a) β-Caryophyllinic acid
(b) Levoglucosan
Concentration (ng m-3)
2.5
2.0
1.5
1.0
0.5
0.0
6.0
4.0
2.0
0.0
Jan
Feb
Mar
Apr
May
Jun
Jul
Aug
Sep
Oct
Nov
Dec
Month

Figure 9.

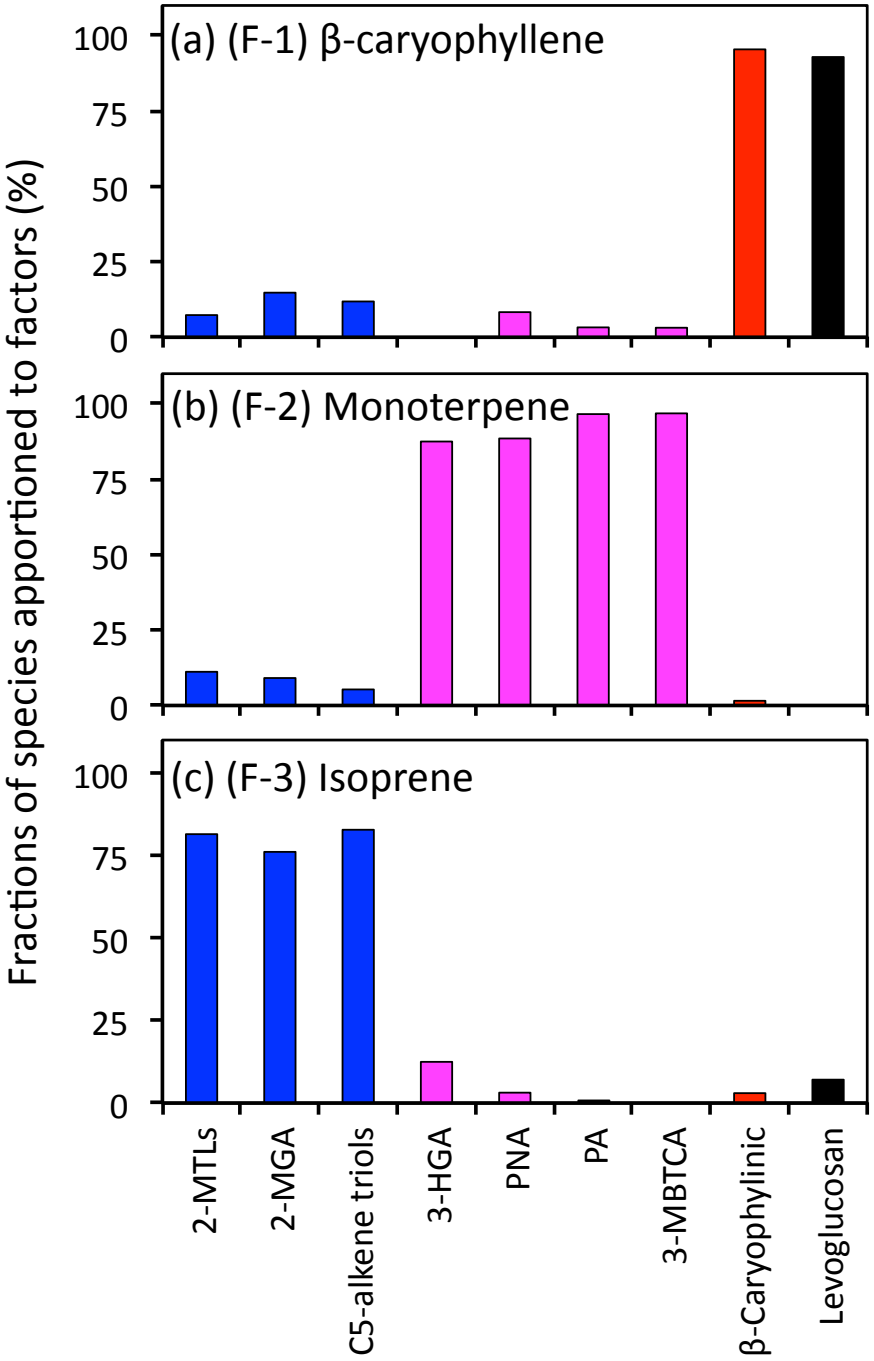
(a) (F-1) β-caryophyllene
(b) (F-2) Monoterpene
(c) (F-3) Isoprene
Fractions of species apportioned to factors (%)
100
75
50
25
0
2-MTLs
2-MGA
C5-alkene triols
3-HGA
PNA
PA
3-MBTCA
β-Caryophylinic
Levoglucosan

1374
1375
1376
1377 Figure 10.
1378

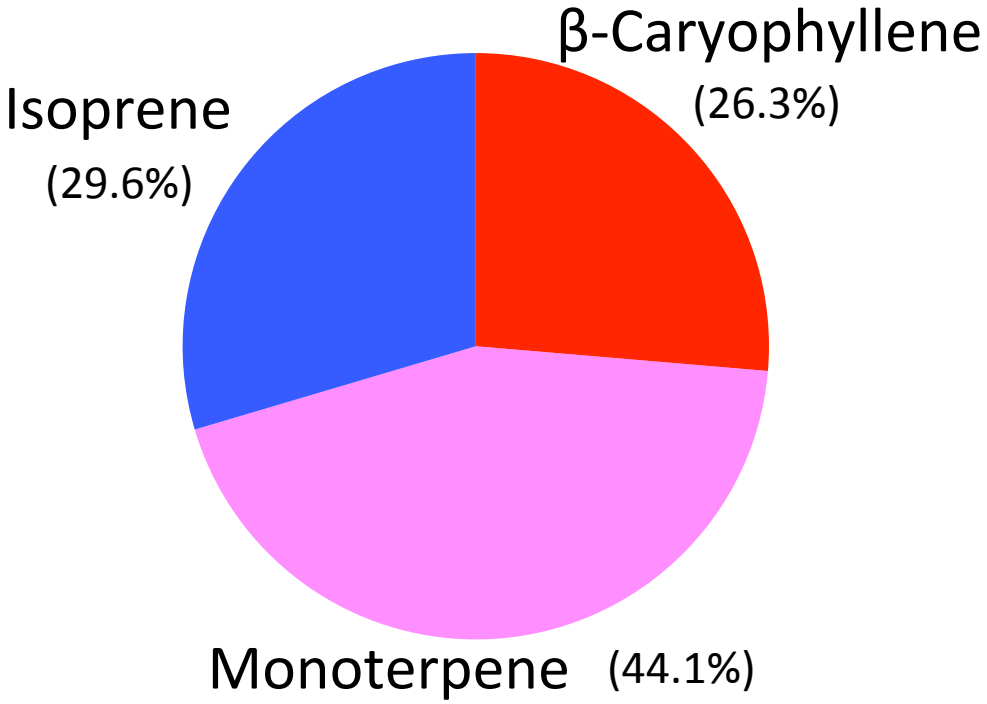

1379
1380